Acknowledgements

This work was supported by Grants-in-Aid for scientific research (15590787) from the Ministry of Education, Culture, Sports, Science and Technology; the Research Grants for Cardiovascular Disease (H13C-1) from the Ministry of Health, Labor and Welfare. The authors thank Orion Pharma, Finland for the supply of entacapone.

References

Akiyama, T., Yamazaki, T., 2001. Myocardial interstitial norepinephrine and dihydroxyphenylglycol levels during ischemia and reperfusion. Cardiovasc. Res. 49, 78–85.

Akiyama, T., Yamazaki, T., Ninomiya, I., 1991. In vivo monitoring of myocardial interstitial norepinephrine by dialysis techniques. Am. J. Physiol. 261, H1643–H1647.

Boulton, A.A., Eisenhofer, G., 1998. Catecholamine metabolism: from molecular understanding to clinical diagnosis and treatment. Adv. Pharmacol. 42, 273–292.

Eisenhofer, G., Goldstein, D.S., Ropchak, T.G., Nguyen, H.Q., Keiser, H.R., Kopin, I.J., 1988. Source and physiological significance of plasma 3,4-dihydroxyphenylglycol and 3-methoxy-4-hydroxyphenylglycol. J. Auton. Nerv. Syst. 24, 1–14.

Eisenhofer, G., Pecorella, W., Pacak, K., Hooper, D., Kopin, I.J., Goldstein, D.S., 1994. The neuronal and extraneuronal origins of plasma 3-methoxy-4hydroxyphenylglycol in rats. J. Auton. Nerv. Syst. 50, 93–107.

Goldstein, D.S., Eisenhofer, G., Stull, R., Folio, C.J., Keiser, H.R., Kopin, I.J., 1998. Plasma dihydroxyphenylglycol and the intraneuronal disposition of norepinephrine in humans. J. Clin. Invest. 81, 213–220.

Illi, A., Sundberg, S., Ojala-Karlsson, P., Korhonen, P., Scheinin, M., Gordin, A., 1995. The effect of entacapone on the disposition and hemodynamic effects of intravenous isoproterenol and epinephrine. Clin. Pharmacol. Ther. 58, 221–227.

Karhunen, T., Tilgmann, C., Ulmanen, I., Julkunen, I., Panula, P., 1994. Distribution of catechol-*O*-methyltransferase enzyme in rat tissues. J. Histochem. Cytochem. 42, 1079–1090.

Lambert, G.W., Kaye, D.M., Vaz, M., Cox, H.S., Turner, A.G., Jennings, G.L., Esler, M.D., 1995. Regional origins of 3-methoxy-4-hydroxyphenylglycol in plasma: effects of chronic sympathetic nervous activation and denervation, and acute reflex sympathetic stimulation. J. Auton. Nerv. Syst. 55, 169–178.

Levin, J.A., 1974. The uptake and metabolism of ^{3}H-L- and ^{3}H-DL-norepinephrine by intact rabbit aorta and by isolated adventitia and media. J. Pharmacol. Exp. Ther. 190, 210–226.

Lindmar, R., Löffelholz, K., 1974. Neuronal and extraneuronal uptake and efflux of catecholamines in the isolated heart. Naunyn-Schmiedeberg's Arch. Pharmacol. 284, 63–92.

Lundvall, J., Edfeldt, H., 1994. Very large range of baroreflex sympathetic control of vascular resistance in human skeletal muscle and skin. J. Appl. Physiol. 76, 204–211.

Männistö, P.T., Kaakkola, S., 1999. Catechol-*O*-metyltransferase (COMT) activity: biochemistry, molecular biology, pharmacology, and clinical efficacy of the new selective COMT inhibitors. Pharmacol. Rev. 51, 593–628.

Scheinin, M., Illi, A., Koulu, M., Ojara-Karsson, P., 1998. Norepinephrine metabolites in plasma as indicators of pharmacological inhibition of monoamine oxidase and catechol *O*-methyltransferase. Adv. Pharmacol. 42, 367–370.

Spraul, M., Anderson, E.A., Bogardus, C., Ravussin, E., 1994. Muscle sympathetic nerve activity in response to glucose ingestion. Impact of plasma insulin and body fat. Diabetes 43, 191–196.

Takauchi, Y., Kitagawa, H., Kawada, T., Akiyama, T., Yamazaki, T., 1997. High-performance liquid chromatographic determination of myocardial interstitial dihydroxyphenylglycol. J. Chromatogr., B, Biomed. Sci. Appl. 693, 218–221.

Tokunaga, N., Yamazaki, T., Akiyama, T., Sano, S., Mori, H., 2003. In vivo monitoring of norepinephrine and its metabolites in skeletal muscle. Neurochem. Int. 43, 573–580.

Tokunaga, N., Yamazaki, T., Akiyama, T., Mori, H., 2003. Detection of 3-methoxy-4-hydroxyphenylglycol in rabbit skeletal muscle microdialysate. J. Chromatogr., B, Biomed. Sci. Appl. 798, 163–166.

Toumainen, P., Reenila, I., Männistö, P.T., 1996. Validation of assay of catechol-*O*-methyltransferase activity in human erythrocytes. J. Pharm. Biomed. Anal. 14, 515–523.

Trendelenburg, U., 1978. The extraneuronal uptake and metablosim of catecholamines in the heart. In: Paton, D.M. (Ed.), The Mechanism of Neuronal and Extranneuronal Transport of Catecholamines. Raven Press, New York, pp. 259–280.

Tsunoda, M., Takezawa, K., Masuda, M., Imai, K., 2002. Rat liver and kidney catechol-*O*-methyltransferase activity measured by high-performance liquid chromatography with fluorescence detection. Biomed. Chromatogr. 16, 536–541.

Yamazaki, T., Akiyama, T., Shindo, T., 1995. Routine high-performance liquid chromatographic determination of myocardial interstitial norepinephrine. J. chromatogr., B, Biomed. Sci. Appl. 670, 328–331.

Dimeric Interaction between the Cytoplasmic Domains of the Na^+/H^+ Exchanger NHE1 Revealed by Symmetrical Intermolecular Cross-Linking and Selective Co-immunoprecipitation†

Takashi Hisamitsu,‡ Tianxiang Pang,‡ Munekazu Shigekawa,§ and Shigeo Wakabayashi*,‡

Department of Molecular Physiology, National Cardiovascular Center Research Institute, Suita, Osaka 565-8565, Japan, and Department of Human Life Sciences, Senri Kinran University, Suita, Osaka 565-0873, Japan

Received April 1, 2004; Revised Manuscript Received June 24, 2004

ABSTRACT: To investigate the oligomeric structure of Na^+/H^+ exchanger 1 (NHE1), permeabilized cells and membranes from cells expressing NHE1 variants were treated with the oxidizing agent Cu^{2+}/*o*-phenanthroline or the bifunctional sulfhydryl reagent methanethiosulfonate. These treatments resulted in symmetrical intermolecular cross-linking at intrinsic (Cys^{794} and Cys^{561}) or 15 exogenous cysteine residues introduced into the distal carboxyl- (C-) terminal cytoplasmic domain (after aa 600) but not at intrinsic Cys^{538} because of masking by its tight association with calcineurin B-homologous protein. Cross-linking was abolished in membranes solubilized with sodium dodecyl sulfate, which dissociates oligomeric NHE1, while it was preserved in those treated with Triton X-100. In addition, treatment with cross-linkers did not produce the tetrameric forms of NHE1 mutants with two cysteine residues. Thus, cross-linking presumably occurs between adjacent C-termini of the NHE1 dimer but not by a stochastic process via random collision of NHE1 molecules. The observations suggest that at least the distal C-termini of the NHE1 dimer are flexible or mobile and are thereby capable of easily making contact with each other over the large cytoplasmic portion of the molecule. Furthermore, co-immunoprecipitation experiments showed that the proximal C-termini (aa 503−580) have a strong propensity to interact directly with each other in parallel. Deletion of aa 562−579 resulted in disruption of disulfide cross-linking between the C-termini and markedly reduced the intracellular pH sensitivity of Na^+/H^+ exchange, suggesting that the dimeric interaction in this region may control the pH-dependent regulation of NHE1.

The Na^+/H^+ exchangers (NHEs,[1] SLC9 family) are electroneutral transporters that catalyze the exchange of Na^+ and H^+ in plasma membranes or other intracellular organellar membranes in various animal species (*1*−*5*). To date, nine NHE isoforms encoded by different genes have been identified in mammalian tissues, and these isoforms are thought to play different roles in various tissues or in various organellar compartments. The first isoform to be cloned, NHE1 (*6*), is expressed ubiquitously in the plasma membranes of essentially all tissues and plays a major role in maintaining pH_i and cell volume homoeostasis. NHE1 consists of two large functional domains, an amino- (N-) terminal membrane domain (~500 amino acids) containing 12 putative membrane-spanning domains and a long carboxyl- (C-) terminal cytoplasmic domain (~300 amino acids). The N-terminal membrane domain catalyzes substrate transport, while the C-terminal domain is involved in regulation (*7*).

The activity of NHE1 is controlled by various extrinsic factors, including growth factors, hormones, and mechanical stimuli, presumably through the H^+-regulatory site (*1*−*6*, *8*). Such pH-dependent regulation is thought to occur through the interaction of the C-terminal domain with various signaling molecules (*1*−*5*). For example, calcineurin B-homologous protein (CHP) was identified as such an accessory protein that associates tightly with NHE1 (*9*). Recently, we reported that CHP serves as an essential cofactor for the physiological Na^+/H^+ exchange activity through interaction with the juxtamembrane region of the C-terminal domain (*10*). Other factors in addition to CHP, including Ca^{2+}/calmodulin (*11*, *12*), an adaptor protein 14-3-3 (*13*), Nck-interacting kinase NIK (*14*), phosphatidyli-

† This work was supported by Grant-in-Aid for Priority Areas 13142210 and Grant-in-Aid 14580664 for Scientific Research from the Ministry of Education, Science, and Culture of Japan, by the promotion of Fundamental Studies in Health Science of the Organization for Pharmaceutical Safety and Research of Japan (Promotion of Fundamental Studies in Health Science), and by Grant nano-001 for Research on Advanced Medical Technology from the Ministry of Health, Labor, and Welfare of Japan. T.P. was supported by a Japan Society for the Promotion of Science Postdoctoral Fellowship.

* To whom correspondence should be addressed. Tel: +81-6-6833-5012. Fax: +81-6-6835-5314. E-mail: wak@ri.ncvc.go.jp.

‡ National Cardiovascular Center Research Institute.

§ Senri Kinran University.

[1] Abbreviations: NHE, Na^+/H^+ exchanger; CHP, calcineurin B homologous protein; pH_i, intracellular pH; CuP, Cu^{2+}/*o*-phenanthroline; MTS-2, 1,2-ethanediylbis(methanethiosulfonate); MTS-6, 1,6-hexanediylbis(methanethiosulfonate); MTS-17, 3,6,9,12,15-pentaoxaheptadecane-1,17-diylbis(methanethiosulfonate); MTSET, 2-(trimethylammonium)ethyl methanethiosulfonate; EIPA, 5-(*N*-ethyl-*N*-isopropyl)-amiloride; DMEM, Dulbecco's modified Eagle's medium; HEPES, 2-[4-(2-hydroxyethyl)-1-piperazinyl]ethanesulfonic acid; Tris, tris(hydroxymethyl)aminomethane; EDTA, ethylenediamine-*N*,*N*,*N*′,*N*′-tetraacetic acid; PBS, phosphate-buffered saline; PAGE, polyacrylamide gel electrophoresis; DTT, dithiothreitol; SDS, sodium dodecyl sulfate; LDS, lithium dodecyl sulfate; aa, amino acid.

10.1021/bi049367x CCC: $27.50
Published on Web 08/04/2004

nositol 4,5-bisphosphate (*15*), and carbonic anhydrase II (*16*), have been reported to associate with NHE1. However, as structural information is extremely limited even for the hydrophilic C-terminal domain, it is still difficult to determine the precise regulatory mechanism.

In addition to its regulatory aspect, NHE is known to exist as an oligomer in the plasma membrane. A previous study (*17*) showed that NHE1 and NHE3 form the homooligomers by interacting via the transmembrane regions in intact cells although the functional unit may still be monomeric. Consistent with this, NHE1 in the placental brush border membranes was detected as a larger form (~205 kDa) cross-linked by disulfide bonds (*18*). In addition, pre-steady-state kinetics revealed that Na^+/H^+ exchange in kidney brush border membrane vesicles exhibits cooperative extracellular Na^+ dependence despite electroneutral exchange, suggesting that NHE may function as an oligomer (*19*−*21*). Electron cryomicroscopy using two-dimensional crystals indicated that the bacterial Na^+/H^+ antiporter NhaA also appears to form dimers (*22*). However, at present, the physiological significance of this oligomerization is not well understood.

In the present study, we analyzed dimeric interactions between the cytoplasmic domains of NHE1. One aim of this study was to elucidate the structural features of the cytoplasmic domains of the NHE1 dimer. The second aim was to determine whether adjacent cytoplasmic domains of the NHE1 dimer interact directly with each other. We found that symmetrical intermolecular cross-linking at native or introduced cysteine residues occurs between the cytoplasmic domains of the NHE1 dimer and that the expressed cytoplasmic domains interact strongly with each other in cells. This is the first report indicating dimeric interaction between adjacent cytoplasmic domains of two NHE1 molecules.

EXPERIMENTAL PROCEDURES

Cell Culture and cDNA Transfection. The exchanger-deficient cell line PS120 and corresponding transfectants were maintained in Dulbecco's modified Eagle's medium containing 25 mM $NaHCO_3$ and supplemented with 7.5% (v/v) fetal calf serum, penicillin (50 units/mL), and streptomycin (50 μg/mL). Cells were maintained at 37 °C in the presence of 5% CO_2. All cDNA constructs were transfected into PS120 cells by the calcium phosphate−DNA coprecipitation technique, and stable clones were selected by repetitive H^+-killing selection procedures as described previously (*7*).

Construction of the NHE1 Mutant Plasmid. The plasmid carrying a cDNA encoding NHE1 containing unique restriction sites cloned into the mammalian expression vector pECE was described previously (*7*). The cDNA construct for NHE1 in which all endogenous cysteine residues were replaced by alanine, designated as Cys-less NHE1, was also described previously (*23*). Construction of plasmids for NHE1 containing point mutations was carried out by a PCR-based strategy using two template plasmids encoding the wild-type or Cys-less NHE1 as described previously (*23*). Similarly, plasmids containing nucleotide sequences corresponding to the hemagglutinin (HA) epitope YPYDVPDYAS or the c-Myc epitope EQKLISEEDL were constructed by inserting PCR fragments produced using antisense primers containing either epitope sequence and a stop codon just after the C-terminus of NHE1 into the appropriate restriction sites of the plasmid containing NHE1 cDNA. Expression vectors for the C-terminal cytoplasmic domain were constructed by a similar PCR-based strategy using HA- or Myc-tagged NHE1 plasmid as a template. The PCR products were inserted into pEGFP-N1 (Clontech, Palo Alto, CA), in which expression of green fluorescent protein (GFP) was blocked by introduction of a stop codon. Constructs were confirmed by sequencing plasmids with an ABI-PRISM DNA sequencer model 3100 (Applied Biosystems, Foster City, CA). In this study, we used the prefix "cl-" for point mutants produced from Cys-less NHE1 as a background.

Cross-Linking between Cysteine Residues of NHE1. For crude membrane preparation, PS120 cells stably expressing the NHE1 variants were grown to confluence on 100 mm culture dishes and collected with a cell scraper into 1.5 mL microtubes. The cells were then washed once with PBS containing 137 mM NaCl, 2.7 mM KCl, 9.6 mM Na_2HPO_4, and 1.5 mM KH_2PO_4 at pH 7.4 and homogenized with a Physcotron for 30 s at 2800 rpm on ice. The homogenates were centrifuged for 5 min at 4000 rpm, and the supernatants were centrifuged again for 15 min at 50000 rpm. The pellets (crude membranes) were resuspended in PBS, and protein content was adjusted to 2−3 mg/mL.

The membranes (1−1.5 mg/mL) were treated with 100 μM CuP for 15 min at 4 °C. To stop the reaction, EDTA (final concentration, 5 mM) was added to the reaction mixture, and then the membranes were dissolved with LDS sample buffer (Invitrogen, San Diego, CA) and subjected to PAGE. For cross-linking experiments on cells, confluent cells were washed twice with 5 mL of PBSCM (PBS containing 0.1 mM $CaCl_2$ and 1 mM $MgCl_2$, pH 7.4) and permeabilized for 15 min on ice with 30 μM β-escin (Sigma, St. Louis, MO) dissolved in medium (120 mM KCl, 2.5 mM $MgCl_2$, and 25 mM HEPES, adjusted to pH 7.2 with KOH) as described previously (*24*). The permeabilized cells were washed to remove β-escin and incubated with 100 μM CuP for 15 min at 4 °C, and the reaction was stopped by treating cells with 10 mM *N*-ethylmaleimide (NEM). In some experiments, cells were treated directly with cysteine cross-linkers MTS-2, MTS-6, or MTS-17 in PBSCM. The resultant cells were solubilized with PBS containing 2% SDS, 20 mM NEM, and 5 mM EDTA, mixed with concentrated LDS sample buffer, and subjected to PAGE.

Immunoprecipitation and Immunoblotting. Cells were transiently transfected with the HA- or Myc-tagged C-terminal cytoplasmic domain of NHE1, and 48 h later cells were solubilized for 20 min on ice with lysis buffer (1% Triton X-100, 5 mM EDTA, 1 mM phenylmethanesulfonyl fluoride, and 1 mM benzamidine in PBS) and then centrifuged at 15000 rpm for 5 min. The supernatant was incubated for 2 h at 4 °C with anti-tag antibody plus 30 μL of protein A−Sepharose beads (Amersham Biosciences Inc., Piscataway, NJ). The beads were washed five times with ice-cold lysis buffer, and proteins were eluted with LDS sample buffer containing 50 mM DTT. After PAGE on 3−8% gradient gels (Invitrogen) or handmade 7.5% gels (Figure 3), proteins were transferred electrophoretically onto poly(vinylidene difluoride) membranes and subjected to immunoblotting with anti-NHE1 (*11*), anti-HA (Santa Cruz Biotechnology Inc., Santa Cruz, CA), or anti-Myc polyclonal antibody (Santa Cruz) as described previously (*11*). Proteins were visualized

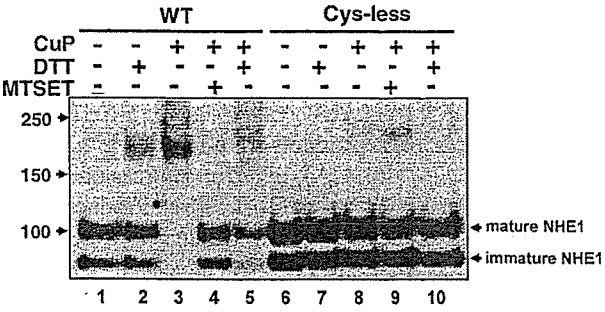

FIGURE 1: Cross-linking of NHE1 proteins with CuP. Crude membranes were prepared from cells expressing wild-type or Cys-less NHE1 and suspended in PBS at a protein concentration of 0.5−1 mg/mL. Membranes (60−90 μg) were treated with CuP (final concentration, 100 μM) for 15 min on ice, and then the reaction was stopped by adding EDTA (5 mM). In some experiments, membranes were briefly (5 min) treated with MTSET (1 mM) before CuP treatment. Samples of 12−18 μg of protein per lane were subjected to PAGE followed by immunoblotting with NHE1-specific antibody under reducing (+DTT) or nonreducing conditions.

by enhanced chemiluminescence detection (Amersham). Data were usually represented as a typical example of three independent experiments.

Measurement of ^{22}Na Uptake. $^{22}Na^+$ uptake activity was measured by the K^+/nigericin pH_i clamp method (*25*). Briefly, serum-depleted cells in 24-well plates were preincubated for 30 min at 37 °C in Na^+-free choline chloride/KCl medium containing 20 mM HEPES/Tris (pH 7.4), 1.2−140 mM KCl, 2 mM $CaCl_2$, 1 mM $MgCl_2$, 5 mM glucose, and 5 μM nigericin (Molecular Probes, Inc., Eugene, OR). $^{22}Na^+$ uptake was started by adding the same choline chloride/KCl solution containing $^{22}NaCl$ (37 kBq/mL; final concentration, 1 mM), 1 mM ouabain, and 0.1 mM bumetanide. In some wells, the uptake solution contained 0.1 mM EIPA. One minute later, cells were rapidly washed four times with ice-cold PBS to terminate $^{22}Na^+$ uptake. pH_i was calculated from $[K^+]_i/[K^+]_o = [H^+]_i/[H^+]_o$ by assuming an intracellular $[K^+]$ of 120 mM. The data were normalized by the protein concentration, which was measured using a bicinchoninic assay system (Pierce Chemical Co., Rockford, IL) using bovine serum albumin as a standard.

RESULTS

Detection of the NHE1 Dimer by Symmetrical Intermolecular Cross-Linking at Cysteine Residues. We first prepared crude membranes from cells expressing NHE1 or its cysteine-free derivative, Cys-less NHE1. Two protein bands were visible on immunoblotting with NHE1-specific antibody (Figure 1, lane 1). The upper band (~100−110 kDa) was the N- and O-linked glycosylated mature form, while the lower band (~80 kDa) was the immature form containing only high-mannose oligosaccharide (*25*). Following treatment of the membranes with the oxidizing agent CuP (100 μM), the NHE1 monomer band disappeared and a new protein band became detectable within the higher molecular mass range of 200−230 kDa, which was twice that of the monomer (Figure 1, lane 3). We also performed similar experiments using membranes pretreated with endoglycosidase F, which is known to cleave N-linked glycans in NHE1 (*26*). Although endoglycosidase F treatment reduced the apparent molecular mass of NHE1 to 92−96 kDa, further

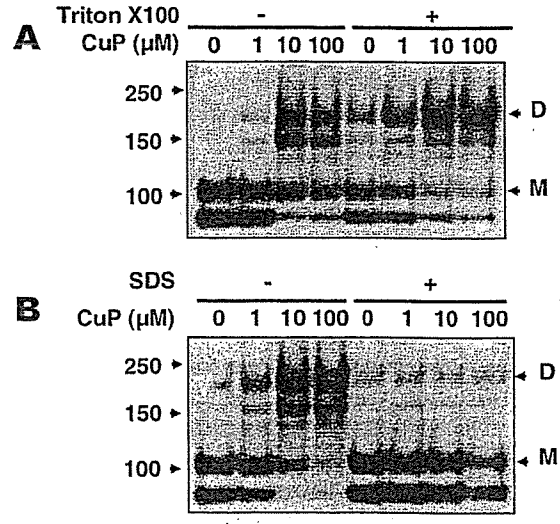

FIGURE 2: Effects of detergents on cross-linking of NHE1 with CuP. Crude membranes from PS120 cells expressing NHE1 were solubilized with or without 1% Triton X-100 (A) or 1% SDS (B). The solubilized membranes were centrifuged at 15000 rpm for 5 min to remove cell debris. Detergent-treated or untreated proteins were incubated with CuP (0−100 μM) for 15 min at 4 °C. After the reaction was stopped with EDTA, proteins were separated on PAGE under nonreducing conditions and subjected to immunoblotting with anti-NHE1 antibody. D and M indicate the positions of the NHE1 dimer and monomer, respectively.

CuP treatment resulted in a similar mobility shift to a higher molecular mass range (175−200 kDa), which was again twice that of the monomer (data not shown). The mobility shift was abolished almost completely by treatment with 10 mM DTT after oxidation or pretreatment with 1 mM cysteine-directed modifier reagent MTSET (Figure 1). In addition, this shift was not observed in Cys-less NHE1 (Figure 1). We also verified that the mature NHE1 expressed in the plasma membrane was cross-linked after surface labeling with NHS-biotin (data not shown). These results suggested that CuP treatment resulted in intermolecular disulfide bond formation at cysteine residues derived presumably from two NHE1 molecules. It should be noted that cross-linking between the immature forms of NHE1 was not detected in this experiment (Figure 1). However, it was often detected when we used membrane preparations including immature forms in relatively high quantities (Figures 2 and 5).

Cross-linking experiments suggested that two NHE1 monomers make contact with each other in the membrane. It is of interest to determine whether their interaction is preserved in the presence of detergents. Membranes were solubilized with 1% Triton X-100 or 1% SDS. After centrifugation the supernatant was treated with CuP and analyzed on immunoblot. As shown in Figure 2, the CuP-induced mobility shift of NHE1 on PAGE occurred in the presence of the relatively mild detergent Triton X-100 but not the more harsh detergent SDS. These findings suggested that two NHE1 monomers are still capable of interacting with each other upon treatment with Triton X-100 but not with SDS. Thus, it is unlikely that disulfide cross-linking is simply dependent on stochastic random collision.

Intermolecular Disulfide Cross-Linking Occurs between Cysteine Residues in Two Adjacent C-Terminal Cytoplasmic Domains of NHE1 Dimers. To identify the cysteine residue(s) that participate in cross-linking, we constructed NHE1

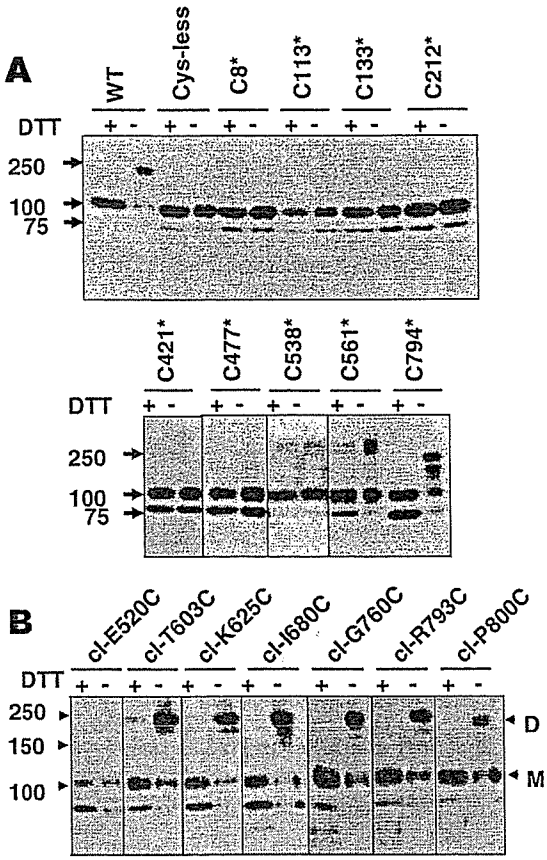

FIGURE 3: Cross-linking of NHE1 proteins containing a single cysteine residue. Crude membranes were prepared from cells stably expressing wild-type, Cys-less, mutants with a single native cysteine residue (A) or mutants with a single cysteine residue introduced into Cys-less NHE1 (B) and treated with 100 μM CuP for 15 min at 4 °C. The resulting membranes were analyzed by immunoblotting with the anti-NHE1 antibody under reducing or nonreducing conditions. Mutants with the native cysteine residue are indicated by an asterisk.

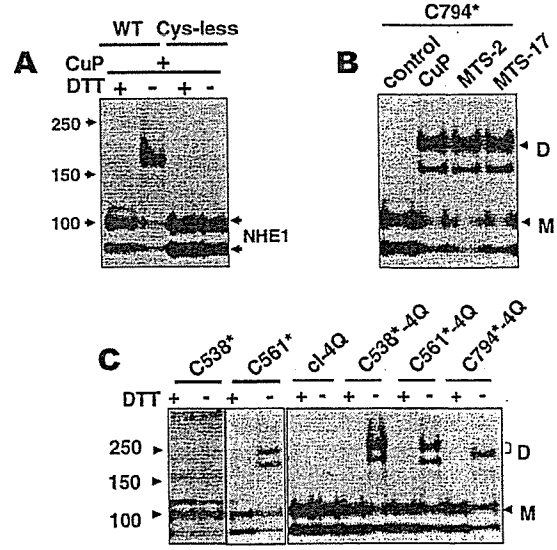

FIGURE 4: Cross-linking of NHE1 and its derivatives in permeabilized cells. (A) Cells stably expressing NHE1 or its Cys-less form were permeabilized with β-escin and then treated with 100 μM CuP for 15 min on ice and analyzed by immunoblotting with anti-NHE1 antibody under reducing and nonreducing conditions. (B) Permeabilized cells stably expressing C794* were treated with CuP, MTS-2, or MTS-17 (100 μM each) for 15 min on ice and analyzed by immunoblotting. (C) Cells stably expressing NHE1 mutants with a native cysteine residue or various derivatives of CHP-binding-defective mutant 4Q were permeabilized with β-escin, then treated with 100 μM CuP for 15 min on ice, and analyzed by immunoblotting with anti-NHE1 antibody. In 4Q, four hydrophobic residues of NHE1, Phe^{526}, Leu^{527}, Leu^{530}, and Leu^{531}, were replaced by four glutamine residues (*10*).

mutants with a single intrinsic cysteine residue using Cys-less NHE1 as the background template plasmid. Disulfide cross-linking with CuP did not occur at Cys^{8} in the cytoplasmic N-tail or at Cys^{113}, Cys^{133}, Cys^{212}, Cys^{421}, or Cys^{477} in the membrane-spanning domains (Figure 3A), consistent with our previous observation that the latter membranous cysteine residues are not accessible to the sulfhydryl reagent biotin maleimide (*23*). In contrast, cross-linking was observed at position 794 in the C-terminal cytoplasmic domain of NHE1 (Figure 3A). Significant but somewhat weaker cross-linking was also observed at position 561 but not at position 538. These results indicated that cross-linking of NHE1 occurs mainly at Cys^{794}. It should be noted that the apparent molecular mass (250 kDa or more) of cross-linked C561* was unexpectedly higher than the calculated mass of the NHE1 dimer. We considered it likely that cross-linking between juxtamembrane cysteine residues of NHE1 leads to a structural change resulting in aberrantly slow migration on PAGE.

We introduced a single exogenous cysteine mutation into several positions of the cytoplasmic domain of NHE1. Surprisingly, in addition to native cysteine residues Cys^{794} and Cys^{561}, CuP induced intermolecular cross-linking at various cytoplasmic amino acid positions, i.e., 603, 625, 680, 760, 793, 800 (Figure 3B), 615, 638, 650, 661, 701, 720, 740, 760, and 780 (data not shown), but not at position 520 (Figure 3B) (see also Figure 10 for amino acid positions in NHE1). We also tested cross-linking with CuP using β-escin-permeabilized cells, which are thought to maintain more nativelike conditions. As shown in Figure 4A, CuP-induced, DTT-dependent cross-linking was observed in permeabilized cells expressing wild-type NHE1 but not Cys-less NHE1. We also detected similar cross-linking in permeabilized cells expressing the NHE1 mutants with exogenous cysteine residues described above (not shown). Using permeabilized cells expressing C794*, we also tested other bifunctional cysteine cross-linkers, MTS-2 and MTS-17, which have spacer lengths of 5 and 25 Å, respectively. These agents were as effective as CuP for cross-linking of C794* (Figure 4B). Thus, the intermolecular cross-linking at cysteine residues from two NHE monomers appears to occur independently of cross-linker spacer length over the large cytoplasmic portion.

We postulated that lack of cross-linking of cysteine residues (positions 520 and 538) in the juxtamembrane domain may be due to the presence of CHP, which was shown to interact strongly with this region (*10*). We constructed several cysteine mutant NHE1s using the Cys-less version of 4Q that was reported previously to abolish CHP binding (*10*). As expected, in contrast to C538* (see Figure 4C), CuP treatment induced cross-linking in cells expressing C538*-4Q as well as other mutants, C561*-4Q and C794*-4Q (Figure 4C), suggesting that cross-linking at position C538 is masked by the presence of bound CHP. It should be noted that the apparent molecular masses for cross-linked products of C538*-4Q and C561*-4Q were higher than that for C794*-4Q (Figure 4C; see also Figure 3).

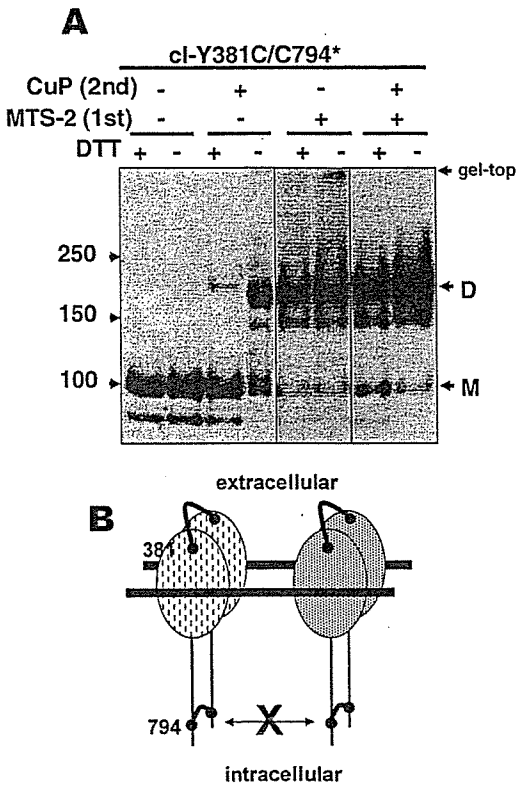

FIGURE 5: Cross-linking of the double-cysteine mutant of NHE1. (A) Cells expressing the NHE1 mutant (cl-Y381C/C794*) with two cysteine residues at positions 381 and 794 were first treated with 100 μM MTS-2 for 15 min on ice, and then crude membranes were prepared. Membranes were further treated with 100 μM CuP for 15 min at 4 °C and analyzed by PAGE under reducing and nonreducing conditions followed by immunoblotting with anti-NHE1 antibody. (B) Schematic drawing showing the possible cross-linking between cysteine residues of two NHE1 monomers.

We further analyzed the oligomerization of NHE1 using cells expressing a mutant with two cysteine residues at amino acid positions 381 and 794; the former (Tyr in wild-type NHE1) is located in the extracellular loop 5 (*23*), while the latter is located in the cytosol. In a preliminary search, we found that cysteines at 381 (and also at 153 and 283) can form intermolecular cross-links on treatment with the uncleavable cross-linker MTS-2. This reagent was not accessible to Cys^{794} from the outside of living cells at least under our experimental conditions (not shown). Treatment of cells expressing this double cysteine mutant with MTS-2 produced the DTT-insensitive protein band at the dimer position on PAGE (Figure 5A, lane 6), suggesting that the intermolecular cross-linking occurred at cysteines introduced into position 381, as shown schematically in Figure 5B. After treatment with MTS-2, crude membranes were prepared. Further treatment of membranes with CuP increased the intensity of the protein band at the dimer position but did not produce the protein band with higher molecular mass corresponding to the tetrameric form (i.e., dimer of dimers) (Figure 5A, lane 8), suggesting that cytoplasmic cross-linking does not occur between dimers cross-linked externally (Figure 5B).

Direct Interaction between the Cytoplasmic Domains of NHE1. Cross-linking experiments suggested that the cytoplasmic domains of NHE1 may be located in close proximity. To test whether the cytoplasmic domains of NHE1 make contact with each other homotypically, we transiently co-expressed two cytoplasmic domains (aa 503−815) with

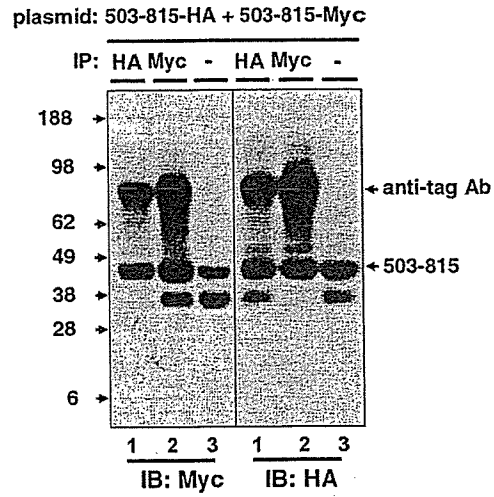

FIGURE 6: Co-immunoprecipitation of the C-terminal cytoplasmic domains of NHE1 labeled with different tags. Two plasmids, 503−815-HA and 503−815-Myc, were transiently cotransfected into PS120 cells. Forty-eight hours after transfection, Triton X-100-solubilized proteins were subjected to immunoprecipitation (IP) with anti-HA or anti-Myc antibodies followed by immunoblotting (IB). Proteins were also analyzed without immunoprecipitation (lanes 3 in both panels).

different tags, HA and Myc, in PS120 cells (see Figure 6). These proteins were expressed well as shown by immunoblotting with each specific antibody, although shorter bands (~35 kDa) were also visible (Figure 6, lane 3 in left and right panels). We observed that the upper bands bind CHP, while the lower bands do not (data not shown). As CHP binds to the juxtamembrane domain (aa 510−540), the former is probably the full-length cytoplasmic domain although its apparent molecular mass (~48 kDa) is higher than the calculated value (~37 kDa), while the latter may be the N-terminally degraded protein. The HA- and Myc-tagged cytoplasmic domain proteins were recovered in the immunoprecipitates with Myc- and HA-specific antibodies (Figure 6, lane 1 in left and lane 2 in right), respectively, suggesting that the two expressed cytoplasmic domains interacted with each other in cells.

Interestingly, tag-specific antibodies did not co-immunoprecipitate the shorter, possibly degraded fragments (Figure 6), suggesting that the N-terminus is important for interaction between the cytoplasmic domains. To identify the site of interaction, we constructed epitope-tagged cytoplasmic domains of different sizes and performed co-immunoprecipitation experiments. Deletion of the N-terminus up to aa 580 abolished co-immunoprecipitation, while deletion up to aa 562 preserved it (Figure 7B). Therefore, at least aa 562−580 is important for the interaction between cytoplasmic domains, but aa 580−815 is not involved. Similar experiments were repeated with combinations of cytoplasmic domains of different sizes. While 562−815-Myc interacted with 503−815-HA, the same protein did not interact with 503−815(Δ562−579)-HA (Figure 8B, parts a and b), indicating that aa 562−579 binds to the same region of the partner protein. Thus, the region 562−579 appears to be crucial for interaction. Furthermore, the cytoplasmic domains deleted of aa 540−579 were also capable of interacting with each other (Figure 8B, part d). In addition, 503−815-Myc interacted with 503−815(Δ562−579)-HA (Figure 8B, part e) and 503−815(Δ540−579)-HA (data not shown). Thus,

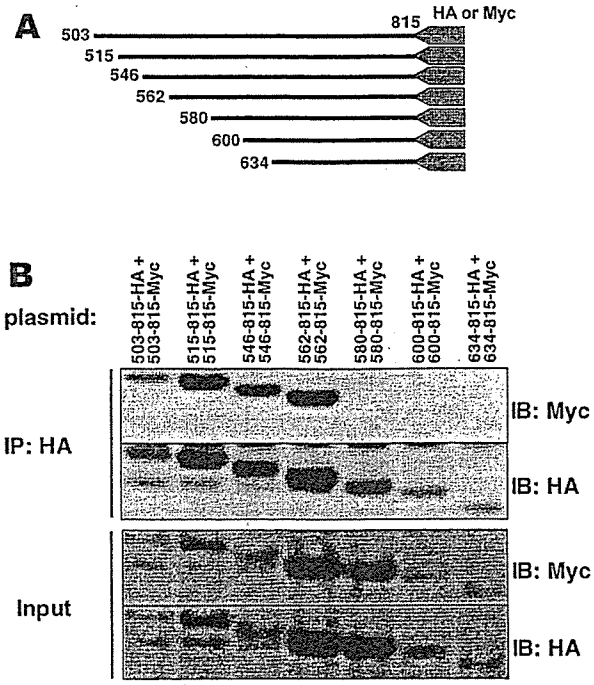

FIGURE 7: Co-immunoprecipitation of the various cytoplasmic domains of NHE1 labeled with different tags. (A) Schematic drawing of cytoplasmic domain constructs. (B) The two plasmids indicated in the figure were transiently transfected into PS120 cells. Triton X-100-solubilized proteins were subjected to immunoprecipitation (IP) with anti-HA antibody followed by immunoblotting (IB) with anti-Myc or anti-HA antibody. Solubilized lysates without immunoprecipitation (input).

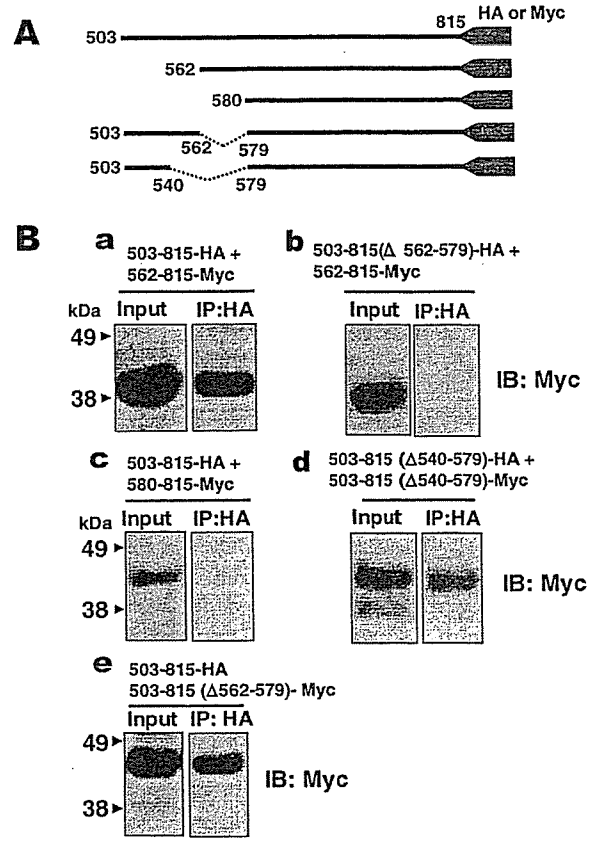

FIGURE 8: Co-immunoprecipitation performed on different combinations of the various cytoplasmic domains of NHE1. (A) Schematic drawing of cytoplasmic domain constructs. (B) The two plasmids indicated in the figure were transiently transfected into PS120 cells. Detergent-solubilized proteins were subjected to immunoprecipitation (IP) with anti-HA antibody followed by immunoblotting (IB) with anti-Myc antibody. Solubilized lysates without immunoprecipitation (input).

in addition to aa 562−579, the more proximal region also has the ability to interact.

We expressed an NHE1 mutant with deletion of part of the cytoplasmic interaction domain (aa 562−579) in PS120 cells and carried out the cross-linking experiment using the crude membrane fraction. In contrast to the appearance of a discrete dimer band for wild-type NHE1, CuP treatment resulted in smears on the gel for Δ562−579 (Figure 9A), suggesting that this mutant protein may form complexes with other cellular proteins through Cys^{794}. Thus, deletion of aa 562−579 markedly inhibited the intermolecular cross-linking between the NHE1 monomers. It should be noted that CuP treatment also produced relatively discrete, cross-linked products with lower molecular mass (~150 kDa), which were presumably derived from the immature form of Δ562−579.

We next measured the EIPA-sensitive $^{22}Na^+$ uptake in transfectants stably expressing wild-type or Δ562−579. Deletion of aa 562−579 reduced the maximal activity at acidic pH_i by about 10-fold (not shown). Furthermore, the same deletion greatly shifted the p*K* value for intracellular pH to the acidic side as compared to wild-type NHE1 (Figure 9B) and abolished NHE1 activation in response to various stimuli, such as growth factors and hyperosmotic stress (data not shown). These observations suggested that this region is critical for preserving the pH-dependent regulation of NHE1.

DISCUSSION

This study was initiated on the basis of our finding that NHE1 in the membranes can be cross-linked with the zero-length cross-linker CuP. Treatment of permeabilized cells or membranes expressing various NHE1 variants with CuP or other MTS reagents resulted in a mobility shift of NHE1 from the monomer to the higher molecular mass range corresponding to the dimer. We also showed that treatment of a double-cysteine mutant NHE1 (positions 381 and 794) with two different cross-linkers did not produce the higher molecular mass products corresponding to the tetrameric form (see Figure 5). The latter observation suggests that two NHE1 dimers are not further cross-linked with each other at the cytoplasmic end. These observations were consistent with the previous findings that treatment of cells with the amino-directed cross-linker disuccinimidyl suberate resulted in production of homodimeric forms of NHE1 or NHE3 (*17*) and that intermolecular disulfide cross-linking of NHE1 occurred in the placental brush border membranes (*18*). A previous study (*17*) indicated that homodimers would be formed somewhere between the N-terminal transmembrane domains of NHE1 (aa 1−500). Unexpectedly, we found that intermolecular cross-linking occurred predominantly at Cys^{794} in the C-terminal cytoplasmic domain, suggesting that, in addition to the transmembrane domain, the two C-termini of the NHE1 dimer might be located in close proximity.

One important observation is that CuP-induced cross-linking of NHE1 occurred even when membranes were solubilized with Triton X-100 (Figure 2A), suggesting that the NHE1 dimer did not dissociate on solubilization with this detergent. Such a strong interaction between monomers was also reported in the bacterial Na^+/H^+ antiporter NhaA,

Original Article

Association of Genetic Polymorphisms of Sodium-Calcium Exchanger 1 Gene, *NCX1*, with Hypertension in a Japanese General Population

Yoshihiro KOKUBO*[1], Nozomu INAMOTO*[1], Hitonobu TOMOIKE*[1], Kei KAMIDE*[2], Shin TAKIUCHI*[2], Yuhei KAWANO*[2], Chihiro TANAKA*[3], Yuki KATANOSAKA*[3], Shigeo WAKABAYASHI*[3], Munekazu SHIGEKAWA*[3], Otosaburo HISHIKAWA*[4], and Toshiyuki MIYATA*[3]

The Na^+/Ca^{2+} exchanger (NCX) is a membrane protein involved in calcium homeostasis, catalyzing the exchange of one Ca^{2+} ion for three Na^+ ions across the cell membrane. The Na^+/Ca^{2+} exchange has been suggested to play a role in the pathogenesis of hypertension. Therefore, we examined whether genetic variations in *NCX1* were associated with hypertension. Among 15 polymorphisms identified in 96 hypertensive subjects by sequencing the entire exon and promoter regions of *NCX1*, 7 representative polymorphisms with a minor allele frequency of greater than 4% were genotyped in 1,865 individuals, of whom 787 were hypertensive and 1,072 were normotensive. These subjects were residents of Suita City and were randomly selected as a population for the Suita cohort study. Multivariate logistic regression analysis performed after adjusting for age, body mass index, hyperlipidemia, diabetes mellitus, smoking, and drinking revealed that the −23200T>C and −23181T>C polymorphisms in the 5′ upstream region of exon 1c were significantly associated with hypertension in men (−23200T>C: CC *vs.* TC+TT: odds ratio=0.61; 95% confidence intervals: 0.39 to 0.97; p=0.04) and in women (−23181T>C: CC *vs.* TC+TT: odds ratio=1.45; 95% confidence intervals: 1.04 to 2.02; p=0.03), respectively. Thus, our study suggests that *NCX1* is one of the genes related to susceptibility to essential hypertension in the Japanese general population.
(*Hypertens Res* 2004; 27: 697–702)

Key Words: NCX1, Na^+/Ca^{2+} exchanger, gene variants, hypertension

Introduction

The Na^+/Ca^{2+} exchanger (NCX) is an important membrane protein involved in calcium homeostasis in various cell types and catalyzes the electrogenic exchange of one Ca^{2+} ion for three Na^+ ions across the plasma membrane (*1–3*). The Na^+/Ca^{2+} exchange has been well demonstrated to play a role in the pathogenesis of hypertension. Blaustein *et al.* suggested that excessive Na^+ retention may secrete an ouabain-like substance that increases the cytosolic Na^+ concentration by inhibiting the plasmalemmal Na^+-pump, which increases the cytosolic Ca^{2+} concentration ($[Ca^{2+}]_i$) by reducing Ca^{2+}-extrusion *via* Na^+/Ca^{2+} exchange (*4–6*). The increase in arteri-

From the *[1]Division of Preventive Cardiology, *[2]Division of Hypertension and Nephrology, and *[3]Research Institute, National Cardiovascular Center, Suita, Japan, and *[4]Suita City Medical Association, Suita, Japan.
This study was supported by the Program for Promotion of Fundamental Studies in Health Science of the Pharmaceuticals and Medical Devices Agency (PMDA) of Japan MPJ-3.
Address for Reprints: Yoshihiro Kokubo, M.D., Ph.D., Division of Preventive Cardiology, National Cardiovascular Center, 5–7–1 Fujishiro-dai, Suita 565–8565, Japan. E-mail: ykokubo@hsp.ncvc.go.jp
Received March 2, 2004; Accepted in revised form June 4, 2004.

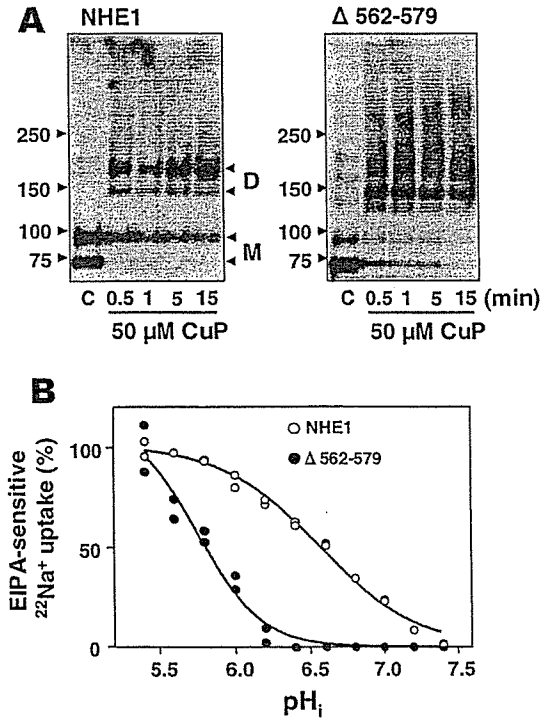

FIGURE 9: Properties of deletion mutant Δ562−579 of NHE1. (A) Membranes were prepared from cells expressing wild-type NHE1 or deletion mutant Δ562−579, then treated with 50 μM CuP for 0.5−15 min on ice, and analyzed by immunoblotting with anti-NHE1 antibody. A typical example of three independent experiments was shown. (B) The pH_i dependence of $^{22}Na^+$ uptake in cells expressing wild-type NHE1 or deletion mutant Δ562−579 was measured as described in Experimental Procedures.

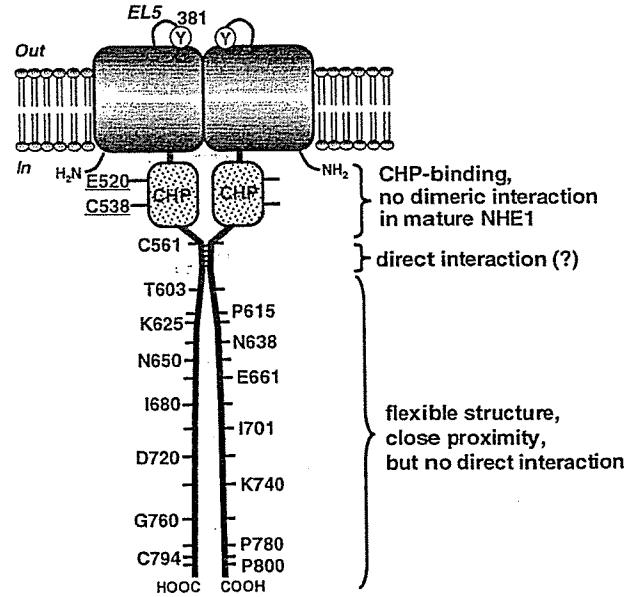

FIGURE 10: Possible dimer model of NHE1. Positions of amino acid residues mutated in this study were indicated. The region aa 562−579 would confer dimerization of the cytoplasmic regulatory domain. Although the region aa 503−540 has also the ability to interact with each other, it would not make contact in the mature NHE1 expressed in the plasma membrane because CHP tighly associates with this region. The distal region (aa 600−815) would have a flexible structure.

which did not dissociate on solubilization with dodecyl maltoside (*27*). However, CuP-induced cross-linking was abolished when membranes were solubilized with the harsher detergent SDS, which is expected to dissociate the NHE1 dimer (Figure 2B). These observations suggest that dimerization is not a stochastic process resulting from random collisions between monomers.

We found that CuP-induced cross-linking of NHE1 occurs predominantly at Cys^{794} and weakly at Cys^{561}. Surprisingly, such symmetrical cross-linking was also observed between almost all cysteine residues introduced into the distal C-terminal region (amino acid positions 615, 625, 638, 650, 661, 680, 701, 720, 740, 760, 780, and 800), suggesting that two C-termini are able to make contact at various cytoplasmic sites, despite the interaction of various signaling molecules with this region of NHE1. This unusual phenomenon, however, does not appear to be due to artifacts resulting from protein denaturation or aggregation because cross-linking at multiple sites also occurred in permeabilized cells which are expected to preserve the relatively intact membrane integrity and because biotin-labeled surface NHE1 proteins were also cross-linked in a similar way (see Results). We observed that CuP-induced cross-linking between Cys^{538} residues does not occur normally but becomes detectable when CHP binding is disrupted by mutation (4Q) (Figure 4D), suggesting that tightly bound CHP sterically blocks the homotypic interaction between CHP-binding domains (aa 510−540) of wild-type NHE1. Although Ca^{2+}/calmodulin (*11*, *12*), 14-3-3 (*13*), tescalcin (*28*, *29*), carbonic anhydrase II (*16*), and heat shock protein (30) were reported to bind to several regions within the distal C-terminal domain, the results of the present study suggest that, unlike CHP, these proteins may interact with NHE1 only in a spatially or temporally restricted fashion.

In addition to CuP treatment, cross-linking at intrinsic or other introduced cysteine residues also occurred upon treatment with the thiol-directed cross-linkers MTS-2 and MTS-17, the spacer arms of which have lengths of 5 and 25 Å, respectively (*31*). These observations strongly suggest that the distal C-terminus of NHE1 has a flexible structure (Figure 10), thereby allowing the distance between the cytoplasmic domains of the NHE1 dimer to change easily. The distal regions thus do not directly interact, consistent with the recent result that the last C-terminal 183 amino acids of NHE1 have only a slight tendency to dimerize on their own (*29*). On the basis of circular dichroism measurements, Li et al. (*29*) reported that the distal region of NHE1 contains essentially a β-sheet, β-turn, and an unstructured part, but almost no α-helix, and that the secondary structure is significantly altered upon changes in pH or Ca^{2+} concentration. The high degree of flexibility of the NHE1 cytoplasmic domain may play an important role in its function. Previously, we proposed that Ca^{2+}-induced activation of NHE1 occurs through derepression of the autoinhibitory domain (aa 635−656) caused by calmodulin binding (*11*, *12*). The mobile cytoplasmic domain might provide structural benefits for such a Ca^{2+}-induced activation because the autoinhibitory domain is predicted to interact with an acceptor region(s) within the transmembrane domain of NHE1 in the resting state and to leave the putative acceptor in response to Ca^{2+} mobilization (*32*). In addition, NHE1 may control actin cytoskeletal reorganization through interaction with ERM family proteins (*33*), thereby regulating stress fiber formation and cell locomotion (*33*−*35*). Two different functions of NHE1, ion exchange and cytoskeletal rearrangement, appear to be regulated independently (*33*−*35*). Flexibility of the

cytoplasmic domain may help to alleviate constraints on the transmembrane ion transport domain, which may be produced by interaction with the cytoskeleton. Some degree of flexibility was also observed in the N-terminal cytoplasmic domain of the anion exchanger AE1 (band 3), which is known to bind the membrane-cytoskeleton anchoring protein ankyrin (*36*, *37*), although this domain of AE1 has a relatively compact dimeric structure (*38*). It is interesting to note that, in contrast to NHE1, intermolecular cross-linking occurs between two different endogenous cysteine residues, Cys^{201} and Cys^{317}, in the cytoplasmic domain of AE1 (*39*).

The structure of the proximal C-terminal region of NHE1 appears to be quite different from the distal end of the molecule. We found that the expressed C-terminal domains interact strongly in cells through several sites within aa 503−580. The requirement of symmetrical regions within aa 503−580 for the interaction (Figure 8) suggests that this homotypic association is specific and not due to nonspecific binding or aggregation. These observations indicate that this region (aa 503−580) of NHE1 has a strong propensity to interact with the same region in adjacent molecules in a parallel fashion. Thus, in addition to the transmembrane domains (*17*), this cytoplasmic region may be another candidate for the dimer interface. However, it was difficult to determine whether these regions of the NHE1 dimer interact when the whole NHE1 is expressed in the plasma membrane. The CuP-induced Cys^{538}-Cys^{538} cross-linking of NHE1 was blocked by tightly bound CHP (Figure 4D). In addition, purified CHP complexed with aa 503−545 of NHE1 was confirmed to be a monomer on gel filtration (*40*). Therefore, at least the N-terminal halves (aa 503−545) in aa 503−580 of NHE1 would not interact with each other in NHE1 expressed in the membrane (Figure 10). However, the C-terminal halves may associate because CuP-induced cross-linking occurred through Cys^{561} (Figure 3B). Thus, the region aa 562−579 may confer dimerization of the cytoplasmic regulatory domain, which in turn appears to bring the remaining distal flexible portion (aa 580−815) of the respective monomers into close proximity of each other. Previously, we reported that deletions of different regions in subdomain I (aa 515−595) of the NHE1 cytoplasmic domain markedly disrupted the NHE1 function, particularly the pH_i sensitivity (*25*). Here, we observed that deletion of aa 562−579 disrupted the intermolecular disulfide cross-linking of NHE1 and shifted the pH_i dependence of the exchange activity to the acidic side (Figure 9), suggesting that deletion-induced inhibition of NHE1 activity may be due to the structural distortion caused by disruption of dimeric interaction in this subdomain. These observations raise the interesting possibility that NHE1 may function as a cooperative dimer in which two subunits are functionally coupled in the regulation of pH_i sensitivity. This was reinforced by our recent finding that intermolecular cross-linking at cysteine residues introduced into the extracellular loop abolished pH_i regulation by NHE1 (T. Hisamitsu, unpublished observations).

It is also possible that the parallel association between the relatively long juxtamembrane regions (aa 503−580) has some other important physiological roles in the function of NHE1. These relatively hydrophobic stretches of two NHE1 monomers may be masked by interacting with each other during biosynthesis of NHE1, thereby passing the "quality control" checkpoint of the endoplasmic reticulum (ER). Control of retention/retrieval in the ER by oligomerization has been demonstrated previously for some membrane proteins, such as ATP-sensitive potassium channels (*41*), γ-aminobutyric acid receptor (*42*), and *N*-methyl-D-aspartate receptor (*43*). Recently, we obtained some evidence that CHP does not bind to the immature form of NHE1 which is retained in the ER (our unpublished results). Therefore, it is plausible that NHE1 and CHP are capable of interacting only after these proteins are separately transported to the plasma membrane. The finding that the immature form of Δ562−579 can be cross-linked (Figure 9) suggests that the more proximal CHP-binding regions may dimerize in the ER but not in the plasma membrane.

In summary, we obtained evidence that the distal C-terminal cytoplasmic regions of the NHE1 dimer are flexible and that they are able to make contact easily, while the proximal regions have the intrinsic ability to interact directly with each other. To date, attempts to crystallize the cytoplasmic domain of NHE1 have been hampered by the high degree of degradation and aggregation of proteins expressed in *Escherichia coli* and other organisms, which may result from the unusual structural properties of the C-terminus. Although future studies are required to elucidate the precise structure, the results of the present study provide basic information regarding the dimeric structure of the C-terminal cytoplasmic domains of NHE1 expressed in living cells.

ACKNOWLEDGMENT

We thank Ms. M. Okubo for technical assistance and Ms. K. Endo for manuscript preparation.

REFERENCES

1. Wakabayashi, S., Shigekawa, M., and Pouysségur, J. (1997) Molecular physiology of vertebrate Na^+/H^+ exchangers, *Physiol. Rev. 77*, 51−74.
2. Orlowski, L., and Grinstein, S. (2004) Diversity of the mammalian sodium/proton exchanger SLC9 gene family, *Pfluegers Arch. 447*, 549−565.
3. Counillon, L., and Pouysségur, J. (2000) The expanding family of eucaryotic Na^+/H^+ exchangers, *J. Biol. Chem. 275*, 1−4.
4. Putney, L. K., Denker, S. P., and Barber, D. L. (2002) The changing face of the Na^+/H^+ exchanger, NHE1: structure, regulation, and cellular actions, *Annu. Rev. Pharmacol. Toxicol. 42*, 527−552.
5. Slepkov, E., and Fliegel, L. (2002) Structure and function of the NHE1 isoform of the Na^+/H^+ exchanger, *Biochem. Cell Biol. 80*, 499−508.
6. Sardet, C., Franchi, A., and Pouysségur, J. (1989) Molecular cloning, primary structure, and expression of the human growth factor-activatable Na/H antiporter, *Cell 56*, 271−280.
7. Wakabayashi, S., Fafournoux, P., Sardet, C., and Pouysségur, J. (1992) The Na^+/H^+ antiporter cytoplasmic domain mediates growth factor signals and controls "H^+-sensing", *Proc. Natl. Acad. Sci. U.S.A. 89*, 2424−2428.
8. Wakabayashi, S., Hisamitsu, T., Pang, T., and Shigekawa, M. (2003) Kinetic dissection of two distinct proton binding sites in Na^+/H^+ exchangers by measurement of reverse mode reaction, *J. Biol. Chem. 278*, 43580−43585.
9. Lin, X., and Barber, D. L. (1996) A calcineurin homologous protein inhibits GTPase-stimulated Na-H exchange, *Proc. Natl. Acad. Sci. U.S.A. 93*, 12631−12636.
10. Pang, T., Su, X., Wakabayashi, S., and Shigekawa, M. (2001) Calcineurin homologous protein as an essential cofactor for Na^+/H^+ exchangers, *J. Biol. Chem. 276*, 17367−17372.
11. Bertrand, B., Wakabayashi, S., Ikeda, T., Pouysségur, J., and Shigekawa, M. (1994) The Na^+/H^+ exchanger isoform 1 (NHE1) is a novel member of the calmodulin-binding proteins, *J. Biol. Chem. 269*, 13703−13709.

12. Wakabayashi, S., Bertrand, B., Ikeda, T., Pouysségur, J., and Shigekawa, M. (1994) Mutation of calmodulin-binding site renders the Na^+/H^+ exchanger (NHE1) highly H^+-sensitive and Ca^{2+} regulation-defective, *J. Biol. Chem. 269*, 13710−13715.
13. Lehoux, S., Abe, J., Florian, J. A., and Berk, B. C. (2001) 14-3-3 binding to Na^+/H^+ exchanger isoform is associated with serum-dependent activation of Na^+/H^+ exchange, *J. Biol. Chem. 276*, 15794−15880.
14. Yan, W., Nehrke, K., Choi, J., and Barber, D. L. (2001) The Nck-interacting kinase (NIK) phosphorylates the Na^+/H^+ exchanger NHE1 and regulates NHE1 activation by platelet-derived growth factor, *J. Biol. Chem. 276*, 31349−31356.
15. Aharonovitz, O., Zaun, H. C., Balla, T., York, J. D., Orlowski, J., and Grinstein, S. (2000) Intracellular pH regulation by Na^+/H^+ exchanger requires phosphatidylinositol 4,5-bisphosphate, *J. Cell Biol. 150*, 213−224.
16. Li, X., Alvarez, B., Casey, J. R., Reithmeier, R. A. F., and Fliegel, L. (2002) Carbonic anhydrase II binds to and enhances activity of the Na^+/H^+ exchanger, *J. Biol. Chem. 277*, 36085−36091.
17. Fafournoux, P., Noël, J., and Pouysséur, J. (1994) Evidence that Na^+/H^+ exchanger isoforms NHE1 and NHE3 exist as stable dimers in membranes with a high degree of specificity for homodimers, *J. Biol. Chem. 269*, 2589−2596.
18. Fliegel, L., Haworth, R. S., and Dyck, J. R. B. (1993) Characterization of the placental brush border membrane Na^+/H^+ exchanger: identification of thiol-dependent transition in apparent molecular size, *Biochem. J. 289*, 101−107.
19. Otsu, K., Kinsella, J., Sacktor, B., and Froehlich, J. P. (1989) Transient state kinetic evidence for an oligomer in the mechanism of Na^+−H^+ exchange, *Proc. Natl. Acad. Sci. U.S.A. 86*, 4818−4822.
20. Otsu, K., Kinsella, J. L., Heller, P., and Froehlich, J. P. (1993) Sodium dependence of the Na^+-H^+ exchanger in the pre-steady state: implications for the exchange mechanism, *J. Biol. Chem. 268*, 3184−3193.
21. Kinsella, J. L., Heller, P., and Froehlich, J. P. (1998) Na^+/H^+ exchanger: proton modifier site regulation of activity, *Biochem. Cell Biol. 76*, 743−749.
22. Williams, K. A. (2000) Three-dimensional structure of the ion-coupled transport protein NhaA, *Nature 403*, 112−115.
23. Wakabayashi, S., Pang, T., Su, X., and Shigekawa, M. (2000) A novel topology model of the human Na^+/H^+ exchanger isoform 1, *J. Biol. Chem. 275*, 7942−7949.
24. Konishi, M., and Watanabe, M. (1995) Molecular size-dependent leakage of intracellular molecules from frog skeletal muscle fibers permeabilized with β-escin, *Pfluegers Arch. 429*, 598−600.
25. Ikeda, T., Schmitt, B., Pouysségur, J., Wakabayashi, S., and Shigekawa, M. (1997) Identification of cytoplasmic subdomains that control pH-sensing of the Na^+/H^+ exchanger (NHE1): pH-maintenance, ATP-sensitive, and flexible loop domains, *J. Biochem. 121*, 295−303.
26. Counillon, L., Pouysséur, J., and Reithmeier, R. A. F. (1994) The Na^+/H^+ exchanger NHE-1 possesses N- and O-linked glycosylation restricted to the first N-terminal extracellular domain, *Biochemistry 33*, 10463−10469.
27. Gerchman, Y., Rimon, A., Venturi, M., and Padan, E. (2001) Oligomerization of NhaA, the Na^+/H^+ antiporter of *Escherichia coli* in the membrane and its functional and structural consequences, *Biochemistry 40*, 3403−3412.
28. Mailänder, J., Müller-Esterl, W., and Dedio, J. (2001) Human homolog of mouse tescalcin associate with Na^+/H^+ exchanger type-1, *FEBS Lett 507*, 331−335.
29. Li, X., Liu, Y., Kay, C. M., Müller-Esterl, W., and Fliegel, L. (2003) The Na^+/H^+ exchanger cytoplasmic tail: structure, function, and interactions with tescalcin, *Biochemistry 42*, 7448−7456.
30. Silva, N. L., Haworth, R. S., Singh, D., and Fliegel, L. (1995) The carboxy-terminal region of the Na^+/H^+ exchanger interacts with mammalian heat shock protein, *Biochemistry 34*, 10412−10420.
31. Green, N. S., Reisler, E., and Houk, K. N. (2001) Quantitative evaluation of the length of homobifunctional protein cross-linking reagents used as molecular rulers, *Protein Sci. 10*, 1293−1304.
32. Wakabayashi, S., Ikeda, T., Iwamoto, T., Pouysséur, J., and Shigekawa, M. (1997) Calmodulin-binding autoinhibitory domain controls "pH-sensing" in the Na^+/H^+ exchanger NHE1 through sequence-specific interaction, *Biochemistry 36*, 12854−12861.
33. Denker, S. P., Huang, D. C., Orlowski, J., Furthmayr, H., and Barber, D. L. (2000) Direct binding of the Na−H exchanger NHE1 to ERM proteins regulates the cortical cytoskeleton and cell shape independently of H^+ translocation, *Mol. Cell 6*, 1425−1436.
34. Denker, S. P., and Barber, D. L. (2002) Cell migration requires both ion translocation and cytoskeletal anchoring by the Na-H exchanger NHE1, *J. Cell Biol. 159*, 1087−1096.
35. Lagana, A., Vadnais, J., Le, P. U., Nguyen, T. N., Laprade, R., Nabi, I. R., Noel, J. (2000) Regulation of the formation of tumor cell pseudopodia by the Na^+/H^+ exchanger NHE1, *J. Cell Sci. 113*, 3649−3662.
36. Blackman, S. M., Hustedt, E. J., Cobb, C. E., and Beth, A. H. (2001) Flexibility of the cytoplasmic domain of the anion exchange protein, band 3, in human erythrocytes, *Biophys. J. 81*, 3363−3376.
37. Zhou, J., and Low, P. S. (2001) Characterization of the reversible conformational equilibrium in the cytoplasmic domain of human erythrocyte membrane band 3, *J. Biol. Chem. 276*, 38147−38151.
38. Zhang, D., Kiyatkin, A., Bolin, J. T., and Low, P. S. (2000) Crystallographic structure and functional interpretation of the cytoplasmic domain of erythrocyte membrane band 3, *Blood 96*, 2925−2933.
39. Thevenin, B. J.-M., B. M. Willardson, S., and Low, P. S. (1989) The redox state of cysteines 201 and 317 of the erythrocyte anion exchanger is critical for ankyrin binding, *J. Biol. Chem. 264*, 15886−15892.
40. Pang, T., Hisamitsu, T., Mori, H., Shigekawa, M., and Wakabayashi, S. (2004) Role of calcineurin B homologous protein in pH regulation by the Na^+/H^+ exchanger 1: Tightly bound Ca^{2+} ions as important structural elements, *Biochemistry 43*, 3628−3636.
41. Zerangue, N., Schwappach, B., Jan, Y. N., and Jan, L. Y. (1999) A new ER trafficking signal regulates the subunit stoichiometry of plasma membrane K (ATP) channels, *Neuron 22*, 537−548.
42. Margeta-Mitrovic, M., Jan, Y. N., and Jan, L. Y. (2000) A trafficking checkpoint controls GABA(B) receptor heterodimerization, *Neuron 27*, 97−106.
43. Pérez-Otaño, I., Schulteis, C. T., Contractor, A., Lipton, S. A., Trimmer, J. S., Sucher, N. J., and Heinemann, S. F. (2001) Assembly with the NR1 subunit is required for surface expression of NR3A-containing NMDA receptors, *J. Neurosci. 21*, 1228−1237.

BI049367X

THE JOURNAL OF BIOLOGICAL CHEMISTRY

Vol. 279, No. 25, Issue of June 18, pp. 26274–26279, 2004
Printed in U.S.A.

Regulatory Roles for APJ, a Seven-transmembrane Receptor Related to Angiotensin-type 1 Receptor in Blood Pressure *in Vivo**

Received for publication, April 14, 2004
Published, JBC Papers in Press, April 15, 2004, DOI 10.1074/jbc.M404149200

Junji Ishida‡§, Tatsuo Hashimoto‡§¶, Yasumi Hashimoto‡§, Shiro Nishiwaki‡§, Taku Iguchi‡§, Shuichi Harada‡§, Takeshi Sugaya‡§, Hitomi Matsuzaki‡§, Rie Yamamoto‡§, Naotaka Shiota‖, Hideki Okunishi‖, Minoru Kihara¶, Satoshi Umemura¶, Fumihiro Sugiyama‡‡, Ken-ichi Yagami**‡‡, Yoshitoshi Kasuya§§, Naoki Mochizuki¶¶, and Akiyoshi Fukamizu‡§‖‖**

*From the ‡Center for Tsukuba Advanced Research Alliance, §Institute of Applied Biochemistry, **Institute of Basic Medical Sciences, ‡‡Laboratory Animal Resource Center, University of Tsukuba, Tsukuba, Ibaraki 305-8577, Japan, the ¶Department of Internal Medicine II, Yokohama City University School of Medicine, Yokohama, Kanagawa 236-0004, Japan, the ‖Department of Pharmacology, Shimane University School of Medical, Izumo, Shimane 693-8501, Japan, the §§Department of Biochemistry and Molecular Pharmacology, Graduate School of Medicine, Chiba University, 1-8-1 Inohana, Chuo-ku, Chiba 260-8670, Japan, and the ¶¶Department of Structural Analysis, National Cardiovascular Center Research Institute, Suita, Osaka 565-8565, Japan*

APJ is a G-protein-coupled receptor with seven transmembrane domains, and its endogenous ligand, apelin, was identified recently. They are highly expressed in the cardiovascular system, suggesting that APJ is important in the regulation of blood pressure. To investigate the physiological functions of APJ, we have generated mice lacking the gene encoding *APJ*. The base-line blood pressure of APJ-deficient mice is equivalent to that of wild-type mice in the steady state. The administration of apelin transiently decreased the blood pressure of wild-type mice and a hypertensive model animal, a spontaneously hypertensive rat. On the other hand, this hypotensive response to apelin was abolished in APJ-deficient mice. This apelin-induced response was inhibited by pretreatment with a nitric-oxide synthase inhibitor, and apelin-induced phosphorylation of endothelial nitric-oxide synthase in lung endothelial cells from APJ-deficient mice disappeared. In addition, APJ-deficient mice showed an increased vasopressor response to the most potent vasoconstrictor angiotensin II, and the base-line blood pressure of double mutant mice homozygous for both APJ and angiotensin-type 1a receptor was significantly elevated compared with that of angiotensin-type 1a receptor-deficient mice. These results demonstrate that APJ exerts the hypotensive effect *in vivo* and plays a counterregulatory role against the pressor action of angiotensin II.

A family of G protein-coupled receptors bind a large variety of ligands and plays an essential role for physiological functions *in vivo* including the maintenance of homeostasis in the cardiovascular system. *APJ* (a putative receptor protein related to the angiotensin-type 1 receptor (AT1))[1] is a G protein-coupled receptor that was isolated from human genomic DNA using the polymerase chain reaction (1). The *APJ* has a 31% amino acid sequence homology with the AT1, but APJ does not display specific binding for angiotensin II, which is the ligand of AT1 and exerts a pressor action in the blood pressure regulation (1). Recently, the endogenous ligand of APJ was identified from bovine stomach, and this peptide was named apelin (for APJ endogenous ligand) (2). APJ and apelin are expressed in several tissues including the cardiovascular and the central nervous systems (3–6), and the structure of APJ and apelin is highly conserved among species, suggesting its important physiological roles.

Intravenous administration of apelin suggested a hypotensive effect in rat (5, 7–9). On the other hand, apelin potently contracts human saphenous vein smooth muscle cells *in vitro* (10), indicating that apelin is a potent vasoconstrictor. Thus, at this moment, the action of apelin in blood pressure regulation is controversial, and it is still unclear whether these actions of apelin are really through APJ because of the absence of specific receptor blocker to clarify the *in vivo* functions of APJ. Therefore, in this study, by using animal models such as APJ-deficient mice, APJ/AT1a double knock-out mice, and spontaneously hypertensive rat and by using endothelial cells from mice, we evaluated the functional importance of apelin-APJ signaling in the blood pressure regulation *in vitro* and *in vivo*.

EXPERIMENTAL PROCEDURES

Gene Targeting and Generation of Mutant Mice—The genomic DNA containing the *APJ* locus were isolated from a phage library from C57BL/6 mice (11) with the human *AT1* cDNA as a probe. To construct a targeting vector for the *APJ* gene, the 156-bp fragment of the mouse *APJ* gene between the NcoI site including the translation initiation codon of the gene and the Csp45I site was replaced with the nuclear localization signal-*lacZ* cassette. The neomycin phosphotransferase (*neo*) gene cassette derived from pMC1neoPolyA (Stratagene) was placed downstream of the nuclear localization signal-*lacZ* gene. The

* This work was supported in part by the 21st Century COE Program, "Research for the Future" Program (The Japan Society for the Promotion of Science Grant JSPS-RFTF 97L00804), a grant-in-aid for Scientific Research on Priority Areas, a grant-in-aid for Scientific Research (A) and a grant-in-aid for Young Scientists (B) from the Ministry of Education, Culture, Sports, Science and Technology of Japan, Research Grant 11C-1 for Cardiovascular Diseases, a grant for Comprehensive Research on Aging and Health from the Ministry of Health, Labor, and Welfare of Japan, the University of Tsukuba Special Research Program, Japan Heart Foundation Research Grant, The Nissan Science Foundation, and Suzuken Memorial Foundation. The costs of publication of this article were defrayed in part by the payment of page charges. This article must therefore be hereby marked "*advertisement*" in accordance with 18 U.S.C. Section 1734 solely to indicate this fact.

‖‖ To whom correspondence should be addressed: Center for Tsukuba Advanced Research Alliance, Institute of Applied Biochemistry, University of Tsukuba, Ibaraki 305-8577, Japan. Tel./Fax: 81-298-53-6070; E-mail: akiff@tara.tsukuba.ac.jp.

[1] The abbreviations used are: AT1, angiotensin-type 1 receptor; WKY, Wistar-Kyoto; SHR, spontaneously hypertensive rat; DMEM, Dulbecco's modified Eagle's medium; NO, nitric oxide; eNOS, endothelial NO synthase; L-NAME, N^G-nitro-L-arginine methyl ester.

6.3-kb XhoI/NcoI fragment and the 1.6-kb Csp45I/Sau3AI fragment of the *APJ* gene were included upstream and downstream of these cassettes, respectively (Fig. 1*A*). Details of the negative selection with the diphtheria toxin-A cassette are described elsewhere (12). The TT2 ES cells were grown on embryonic fibroblast feeder cells as described previously (13). Homologous recombination in TT2 ES cells was detected by Southern blotting using probe a (687-bp BanIII-Sau3AI fragment). Chimeric mice were generated by injecting the ES cells into ICR 8-cell embryos (13, 14). AT1a-deficient mice were generated as described previously (11). Double knock-out mice for *APJ* and *AT1a* used in this study were generated from heterozygous mice after the crossing of single APJ-deficient and AT1a-deficient mice.

RNA Preparation and Northern Blot Analysis—Total RNA was isolated from the heart and lung of four independent age-matched mice using ISOGEN (NipponGene) (15). Fifteen micrograms of RNA were denatured with glyoxal, separated by electrophoresis, and transferred to a nylon membrane. The 728-bp NcoI/NaeI fragment that corresponds to the coding regions of *APJ* was used as the APJ receptor-specific probe (probe b). Probes for mouse glyceraldehyde-3-phosphate dehydrogenase were described previously (16).

Measurement of Blood Pressure—The heart rate and systolic, mean, and diastolic blood pressures were measured by a programmable sphygmomanometer (BP-200, Softron, Japan) using the tail cuff method as described previously (17). Unanesthetized mice were introduced into a holder mounted in a thermostatically controlled warning plate and maintained at 37 °C during measurement.

Intraperitoneal Injection of Apelin—Experiments were performed using 4-month-old male mice under the conscious and unrestrained conditions. [Pyr^1]Apelin-13 (Peptide Institute 4361-v) was suspended in saline (0.9% NaCl in distilled water). After the measurement of the basal systolic blood pressure, [Pyr^1]apelin-13 was administered by intraperitoneal injection at 285 μg/kg body weight and the systolic blood pressure was measured continuously. The data were calculated at 5-min intervals for 20 min after the administration of apelin.

Intravenous Injection of Apelin in Wistar-Kyoto (WKY) Rat and SHR—SHR and WKY rats at 12 weeks of age were anesthetized with sodium pentobarbital (35 mg/kg intraperitoneal). PE-10 catheters (Clay Adams, Parsippany, NJ) were inserted into the right femoral artery for measuring blood pressure and into the right femoral vain for allowing the administration of [Pyr^1]apelin-13. The arterial catheter was connected to a pressure transducer (TP-200T, Nihon Kohden, Tokyo, Japan), and blood pressure was measured continuously. The anesthetic level was maintained by subcutaneous injection of 10 mg/kg pentobarbital every 40 min. [Pyr^1]Apelin-13 dissolved in 0.1 ml of saline was administered through the vein catheter (2, 4, and 10 nmol/kg).

Pretreatment with N^G-Nitro-L-Arginine Methyl Ester (L-NAME) and Intraperitoneal Injection of Apelin in Wild-type and APJ-deficient Mice—Experiments were performed using 4-month-old male mice under the conscious and unrestrained conditions. L-NAME (Sigma) was suspended in saline. Systolic blood pressure was continuously measured before and after acute intraperitoneal injection of L-NAME (10 mg/kg body weight). At 15 min after the administration of L-NAME, the additional administration of [Pyr^1]apelin-13 (285 μg/kg body weight) or saline alone was performed by intraperitoneal injection and the systolic blood pressure was measured continuously. The maxima of systolic blood pressure responses to injections of apelin were calculated in a 0–5 min-post-injection of apelin.

Preparation of Endothelial Cells from Wild-type and APJ-deficient Mice—The lung of wild-type and APJ-deficient male mice at 11 weeks of age was perfused with 0.25% heparin/phosphate-buffered saline(−) and removed aseptically, rinsed in 0.25% heparin/phosphate-buffered saline(−), minced into ~1 × 2-mm squares, and digested in 20 ml of collagenase type I (4 mg/ml, Worthington) in serum-free DMEM containing antibiotic at 37 °C for 60 min with shaking. The cellular digest was filtered through a sterile 40-μm nylon mesh and washed in 20 ml of serum-free DMEM, and the cell pellet was resuspended in 4 ml of serum-free DMEM. 2 ml of cell suspension were put into the tube containing 12 ml of 30% Percoll and centrifuged at 800 × *g* for 15 min. 2 ml of the concentrated fraction with the endothelial cells were recovered to which 2 ml of serum-free DMEM were added, and then the Percoll density gradient centrifugation was carried out again. The collected endothelial cells then were resuspended in 4 ml of growth medium (DMEM containing 10% fetal bovine serum and endothelial cell growth supplement from bovine neural tissue (Sigma)) for culture. Contaminated vascular smooth muscle cells were stripped off physically as necessary. Confluent cells were passed routinely at a split ratio of 1–3 after trypsin/EDTA digestion and cultured under the same conditions. We ascertained the purity of endothelial cells by Western blotting with monoclonal anti-mouse CD-31 antibody (BD Biosciences) (data not shown).

Detection of Endothelial NO Synthase (eNOS) Phosphorylation—Isolated endothelial cells from wild-type and APJ-deficient mice were cultured in 6-well plates and stimulated by [Pyr^1]apelin-13 (10 μM) or fetal bovine serum (10%) for 5 min, and the reaction was terminated by adding Laemmli buffer. The cell lysates were subjected to SDS/7.5% polyacrylamide gel electrophoresis and then transferred to polyvinylidene difluoride membrane (Millipore). After blocking with a blocking buffer containing 5% milk, the membrane was incubated with a polyclonal anti-human phospho-eNOS (Ser^{1177}) antibody (Cell Signaling Technology) and bound antibody was detected by horseradish peroxydase-labeled donkey anti-(rabbit IgG) serum (Amersham Biosciences) using Western Lightning Plus chemiluminescence reagents (Perkin-Elmer Life Sciences) to measure the phosphorylation of eNOS. After washing with a reprobing buffer of the composition (62.5 mM Tris-HCl (pH 6.7), 100 mM β-mercaptoethanol, and 2% SDS), the same membrane was subjected to Western blotting with a monoclonal anti-eNOS antibody (BD Transduction Laboratories) to detect the expression levels of eNOS as an internal control.

Treatment with Captopril and Intraperitoneal Injection of Angiotensin II—Systolic blood pressure was measured in conscious and unrestrained female mice at 4 months of age as mentioned above. The basal systolic blood pressure and the pressure responses against intraperitoneal injection of angiotensin II (10 and 30 μg/kg) were measured prior to the administration of captopril. After the administration of captopril (500 mg/liter in drinking water) for 1 week to inhibit the endogenous production of angiotensin II, the pressure responses to angiotensin II given from lower dose (3–30 μg/kg) were recorded continuously for 40 min after the administration of angiotensin II.

Statistical Analysis—The data were analyzed by Student's *t* test for unpaired values. $p < 0.05$ was considered significant. Results are expressed as the means ± S.E.

RESULTS AND DISCUSSION

Generation of APJ-deficient Mice—To generate a null mutation at the mouse *APJ* gene locus, we designed a targeting vector that would replace a portion of the *APJ* coding region with the promoterless *lacZ* gene (Fig, 1*A*). After electroporation of TT2 cells with the targeting vector, homologous recombination was confirmed by Southern blotting (Fig. 1*B*, *left panel*). 10 independent cell lines of 195 G418-resistant cells had undergone homologous recombination at the mouse *APJ* locus. Eight clones were injected into ICR 8-cell embryos to generate chimeric mice, and two clones gave rise to germ line transmission by backcross mating with C57BL/6J mice. The heterozygous mice were intercrossed to produce homozygous offspring, and the mutation at *APJ* loci was detected by Southern analysis of tail DNA (Fig. 1*B*, *right panel*). Of the 396 offspring analyzed, 76 (19%) were homologous for the disrupted allele and 103 (26%) were wild type, indicating the normal embryonic development of the homozygous mutant mice. The histological sections of heart, lung, kidney, spleen, brain, ovary, skeletal muscle, liver, and white adipose did not reveal any differences in morphology between wild-type and heterozygous or homozygous mutant mice (data not shown). In the following study, to gain the equivalent effects of other gene backgrounds with the exception of for the *APJ* gene, we used these intercrossed littermates of heterozygous mice for further physiological experiments.

RNA Analysis—To determine whether *APJ* message was present in homozygous mutants, we performed Northern blot analysis of heart and lung RNA. Although heart and lung highly express the *APJ* gene in rodents (3), homozygous mutant mice had no detectable *APJ* message (Fig. 1*C*). A duplicate blot was analyzed with a glyceraldehyde-3-phosphate dehydrogenase probe to confirm that the RNA sample was intact. These results indicated that *APJ* transcripts were absent completely from homozygous mutant mice (APJ-deficient mice).

Measurement of Blood Pressure and Administration of Apelin—To ascertain whether APJ-mediated pathways participate in the regulation of the cardiovascular system, we measured the systolic blood pressure and heart rate under the steady

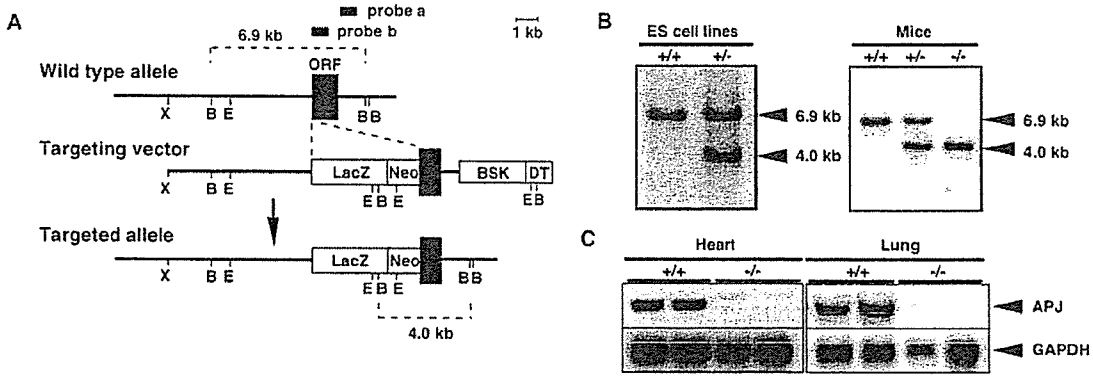

FIG. 1. **Targeted disruption of the mouse APJ gene by homologous recombination in ES cells and mice.** *A*, structure of the targeting vector and partial restriction map of the mouse APJ gene locus before and after targeting event. The intronless open reading frame (*ORF*) is shown as a *closed box*, and the nuclear localization signal-β-galactosidase gene (*LacZ*), the neomycin phosphotransferase gene (*Neo*), the diphtheria toxin-A gene (*DT*), and pBluescript II (*BSK*) are shown as an *open box*. The position of the probes used for Southern blot analysis (*closed bar*) is also shown. The restriction sites used are: *B*, BamHI; *E*, EcoRI; *X*, XhoI. *B*, Southern blot analyses of ES cell (*left panel*) and representative litter derived from a heterozygous intercross (*right panel*). Genomic DNAs isolated from wild type (+/+) and targeted (+/−) ES cell clones and from tails of wild-type (+/+), heterozygous (+/−), and homozygous (−/−) APJ mutant mice were digested with BamHI, electrophoresed, and blotted. Fragments obtained from wild type (6.9 kb) and targeted alleles (4.0 kb) were detected by *probe a*. *C*, Northern blot analysis of APJ-deficient mice. RNA samples from heart and lung of wild-type (+/+) and homozygous (−/−) mutant mice were electrophoresed and subjected to Northern blot analysis with probes for mouse APJ (*probe b*) and glyceraldehyde-3-phosphate dehydrogenase.

state. As shown in Fig. 2*A*, APJ-deficient mice and wild-type mice did not show any difference in the base-line systolic blood pressure (106.7 ± 2.0 and 105.9 ± 2.5 mm Hg, respectively) and the heart rate (632.0 ± 19.2 and 616.1 ± 32.8 cpm, respectively), suggesting that APJ is not essential for the maintenance of base-line blood pressure. Furthermore, it is reported that apelin is concerned in the regulation of drinking behavior (5, 7, 18), but the volume of water intake and the concentration of urinary electrolytes of APJ-deficient mice are not distinguishable from those of wild-type littermates when water is freely available (data not shown).

It has been reported that blood pressure was decreased transiently by the systemic administration of apelin, the endogenous ligand of APJ, in rat (5, 7–9). We administered apelin to APJ-deficient mice to ascertain whether these actions of apelin are really through APJ. Apelin is derived from a 77-amino acid precursor and processed to several isoforms by deleting the amino terminus (3, 4). The pyroglutamylated form of apelin-13, [pGlu]apelin-13, has been reported to have the effective activity at the receptor *in vitro* (3). Conscious male mice were intraperitoneally injected with [pGlu]apelin-13. The acute administration of apelin transiently and significantly decreased in the systolic blood pressure of wild-type mice (Fig. 2*B*). On the other hand, the apelin injection revealed no change in systolic blood pressure of APJ-deficient mice (Fig. 2*C*) without a change in heart rate as well as that of wild-type mice (data not shown). These results clearly demonstrate that the systemic administration of apelin lowers the blood pressure in wild-type but not in APJ-deficient mice and that APJ is really responsible for this action of apelin on the blood pressure regulation.

Administration of Apelin to Spontaneously Hypertensive Rat—Given that the activation of the apelin-APJ signaling pathways lowers the blood pressure under the steady state in mice (Fig. 2*B*) and rats (5, 7–9), is the hypotensive effect also evoked in the hypertensive conditions? To address this question, we administered apelin intravenously to a chronic hypertensive model animal, SHR, and measured continuously the arterial blood pressure. WKY rats were used as a control. Before the administration of apelin, the base-line mean blood pressure of WKY rats and SHR was measured (77 ± 4 mm Hg, n = 10, and 117 ± 2 mm Hg, n = 9, respectively). When apelin was injected into the normotensive WKY rats, a dose-dependent and significant decrease in mean arterial blood pressure was elicited (Fig. 2*D*, *closed bar*) as reported previously (5, 7–9). The intravenous administration of apelin to SHR was found to significantly lower the mean arterial blood pressure in a dose-dependent manner (Fig. 2*D*, *open bar*). Thus, the hypotensive effect by the systemic administration of apelin was evoked in hypertensive animals, but the degree of decrement was less than that of WKY rats. The effects of apelin on blood pressure regulation in the hypertensive model animals have not been explored previously to date, although it has been recently reported that apelin-APJ signaling pathways were down-regulated in the mechanical stretch models *in vitro*, in the animal models of chronic ventricular pressure overload, and in patients with chronic heart failure *in vivo* (19–21). In addition, the angiotensin-converting enzyme-related carboxypeptidase (ACE2), a zinc metalloprotease whose closest homolog is the angiotensin I-converting enzyme, was identified as the breakdown enzyme for apelin peptides (22). The reduction of apelin-induced hypotensive effects in SHR compared with WKY rats might be attributed to the differences in the balance of the production and degradation of apelin and in the sensitivity of APJ-mediated intracellular signalings including receptor desensitization.

Effects of a Nitric Oxide Synthase Inhibitor on the Action of Apelin Administration—Tatemoto *et al.* (8) suggest that apelin causes vasodilatation via the activation of the nitric oxide (NO)/L-arginine system. NO generated by eNOS has a central role in the regulation of vascular tone. Therefore, we examined the effects of a nitric-oxide synthase inhibitor, L-NAME, against the depressor response of apelin-APJ signaling observed in wild-type mice. After a single intraperitoneal bolus injection (10 mg/kg body weight) of L-NAME, the systolic blood pressure increased similarly from 111.0 ± 2.2 to 142.3 ± 2.9 mm Hg and from 108.1 ± 2.4 to 142.4 ± 2.5 mm Hg in wild-type and APJ-deficient mice (n = 7–8/group), respectively. This increase in systolic blood pressure with the administration of L-NAME was described previously in rat, and the systolic blood pressure of each group reached a plateau at around 10 min after administration (data not shown). Accordingly, we injected the apelin peptide at 15 min after L-NAME administration. The injection of apelin induced an acute and transient decrease in systolic blood pressure in the non-treated wild-type mice. In contrast, the administration of the same dose of apelin caused almost no change in systolic blood pressure in wild-type mice pretreated

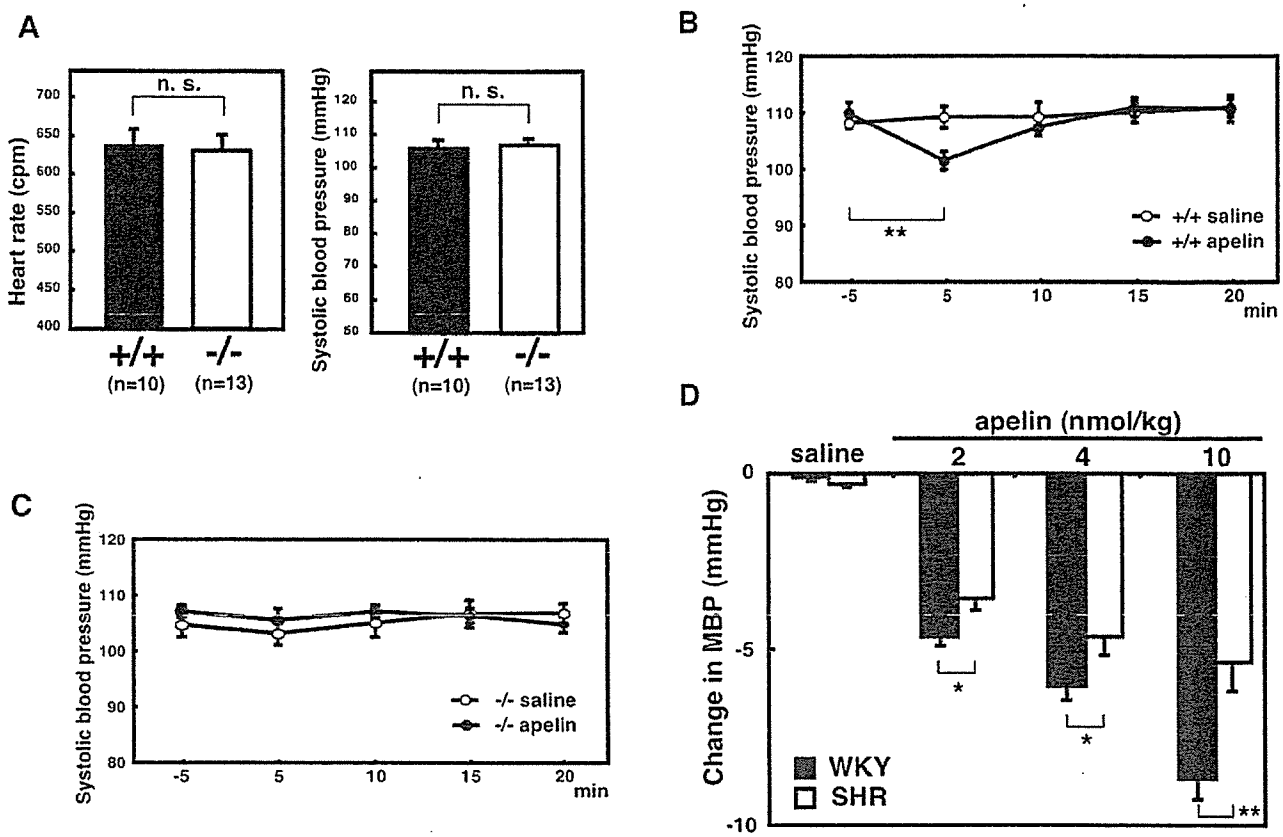

FIG. 2. **Measurement of heart rate and blood pressure and administration of apelin to APJ mutant mice and SHR.** *A*, heart rate (in cpm) and systolic blood pressure (in mm Hg) values of 2–4-month-old wild-type (+/+) and APJ-deficient (−/−) mice under the steady state. *n*, total number of mice; *n.s.*, not significant. *B* and *C*, effects of intraperitoneal apelin ([Pyr^1]apelin-13) and saline (control) injection to wild-type mice (*B*) or APJ-deficient mice (*C*) on systolic blood pressure. Data were calculated at 5-min intervals for 20 min after the administration of [Pyr^1]a pelin-13. *Open circles*, the saline administration; *filled circles*, apelin administration (n = 8/group). *D*, effect of apelin administration on mean blood pressure in WKY Rat and SHR. [Pyr^1]Apelin-13 was injected intravenously to the rats at the doses of 2, 4, and 10 nmol/kg (n = 8–10/group). *Filled bars*, WKY rat; *open bars*, SHR; *Change in MBP*, change in mean blood pressure. Data are means + S.E. *, $p < 0.05$; **, $p < 0.01$ by unpaired Student's t test.

with L-NAME (Fig. 3*A*, *closed bar*). The systolic blood pressure in APJ-deficient mice was not changed by the apelin peptide injection regardless of L-NAME administration (Fig. 3*A*, *opened bar*), suggesting that the suppressive action point of L-NAME against the hypotensive effect observed in wild-type mice by apelin injection exists under the APJ-mediated signalings. Tatemoto *et al.* (8) also report that the systemic administration of apelin significantly increased the plasma NOx concentration in rats, whereas the increase in the NOx concentration was not observed in the rats pretreated with L-NAME. These findings provided a possibility that the depressor action of apelin-APJ signaling is the result of stimulation of the NO production.

Apelin-mediated Ser^{1176} eNOS Phosphorylation in Endothelial Cells from Mice—NO produced by eNOS has a crucial role in the regulation of vascular tone. It was reported that eNOS is activated by a variety of physiological and pathophysiological stimuli, including hormones and growth factors, and by mechanical stimuli. eNOS is activated by phosphorylation at the Ser^{1177} residue (based on the human eNOS sequence and is equivalent to bovine eNOS-Ser^{1179} and mouse eNOS-Ser^{1176}), the best characterized eNOS phosphorylation site, that is phosphorylated by protein kinase Akt, a downstream mediator of phosphatidylinositol 3-kinase, and greatly contributes to the eNOS activation (23–25). To determine whether apelin-APJ signaling can actually activate eNOS, the endothelial cells derived from wild-type and APJ-deficient mice were stimulated with apelin and phosphorylation of eNOS at Ser^{1176} residue was assessed by using a phosphorylation state-specific eNOS antibody. As shown in Fig. 3*B*, eNOS in the endothelial cells from wild-type and APJ-deficient mice was activated significantly by serum stimulation (*gray bar*) compared with non-treated cells (*open bar*). Interestingly, eNOS Ser^{1176} phosphorylation by apelin stimulation was promoted in wild-type endothelial cells but not in APJ-deficient endothelial cells (*closed bar*). This is the first report that apelin can activate eNOS in endothelial cells and that APJ plays a critical role in apelin-induced phosphorylation of eNOS, which potentializes the hypotensive effect on blood pressure regulation.

Association of Mouse APJ with Pressor Action of Angiotensin II—In blood pressure regulation, the vasoconstriction and vasorelaxation systems constantly antagonized each other to maintain normal blood pressure. To test whether APJ plays a role in blood pressure regulation as a counterregulatory component against vasopressor actions, we performed the systemic angiotensin II administration and measured the systolic blood pressure of wild-type and APJ-deficient mice. The intraperitoneal injection of pharmacological doses of angiotensin II (10 and 30 μg/kg) resulted in a similar increase in systolic blood pressure in both groups (Fig. 3*A*), suggesting that the pressor response mediated by AT1 in the steady state was not affected by the disruption of the *APJ* gene.

We next used a different protocol for angiotensin II administration to clarify the APJ function in blood pressure regulation. Hein *et al.* (26) previously evaluated the role of angioten-

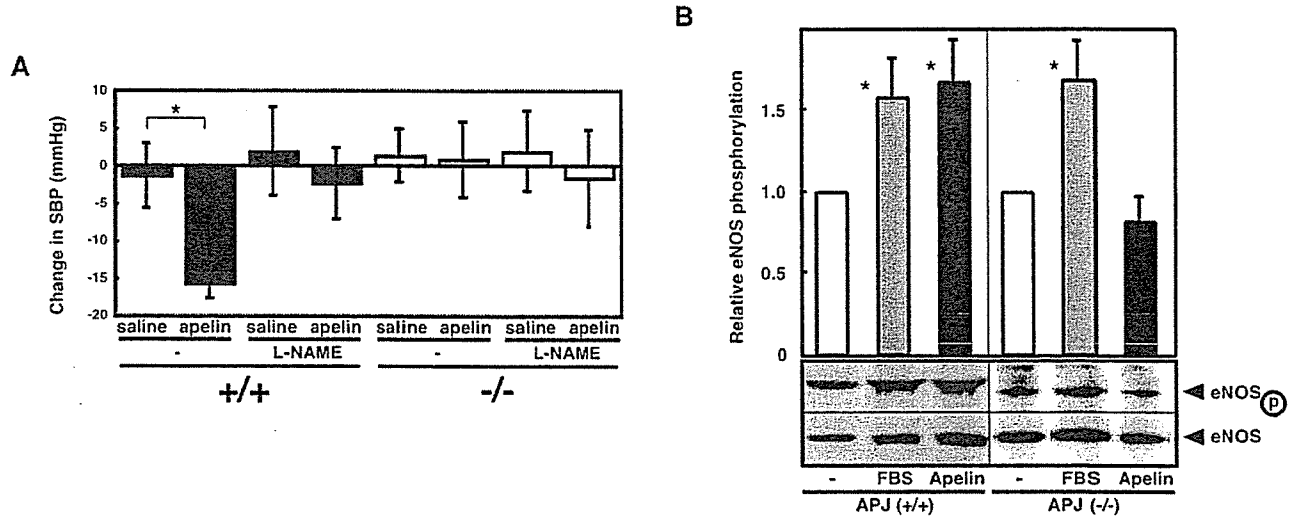

FIG. 3. **Effect of L-NAME pretreatment on apelin-induced blood pressure responses and activation of eNOS in endothelial cells from mice.** *A*, apelin was injected to the wild-type mice (*filled bar*) and APJ-deficient mice (*open bar*) with or without pretreatment of L-NAME (n = 7–8/group). *Change in SBP*, change in systolic blood pressure. Data are means ± S.E. *, $p < 0.05$ by unpaired Student's t test. *B*, apelin stimulates phosphorylation of eNOS at the Ser^{1176} residue. Isolated endothelial cells from wild-type and APJ-deficient mice were treated with apelin or fetal bovine serum (*FBS*) for 5 min. Cell lysates were prepared and analyzed by Western blotting. The membrane was first probed with anti-phosphorylated eNOS antibody (*eNOS-p*) and then successively with anti-eNOS antibody after stripping (*eNOS*). The ratio of the intensity of phosphorylated eNOS to that of eNOS (*eNOS-p/eNOS*) was determined using NIH image, and the ratio of the sample with no stimulation was taken as 1.0. Representative results are shown for three independent experiments. Data are means ± S.E. *, $p < 0.05$ compared with control.

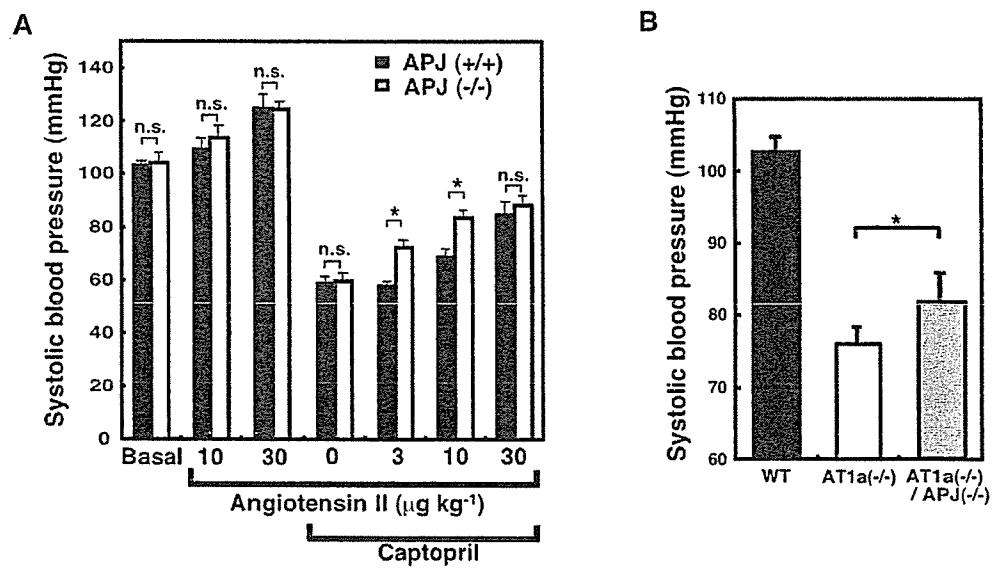

FIG. 4. **Association of mouse APJ with pressor action of angiotensin II.** *A*, systolic blood pressure responses of wild-type and APJ-deficient mice by the administration of angiotensin II. Systolic blood pressures in the 5-min postinjection of angiotensin II were indicated. *Filled bars*, wild-type (+/+) mice; *open bars*, APJ-deficient (−/−) mice; *Captopril*, the administration of an angiotensin-converting enzyme inhibitor to prevent endogenous production of angiotensin II; *Basal*, systolic blood pressure prior to the administration of captopril. *B*, base-line systolic blood pressure in 3-month-old wild-type (*closed bar*), AT1a-deficient (*open bar*), and double mutant mice homozygous for both APJ and AT1a (*grayed bar*) under conscious conditions (n = 12–17/group). Data are means ± S.E. *, $p < 0.05$; **, $p < 0.01$ by unpaired Student's t test.

sin-type 2 receptor (AT2) in blood pressure regulation as a counterregulatory component against vasopressor actions by administrating captopril to AT2-deficient mice. We pretreated mice with captopril, the inhibitor of angiotensin-converting enzyme, for 1 week to block the production of endogenous angiotensin II and then continuously injected lower and more physiological doses of angiotensin II. The captopril-treated wild-type mice revealed an increased systolic blood pressure by the intraperitoneal injection of angiotensin II (above 10 μg/kg). On the contrary, the captopril-treated APJ-deficient mice revealed a significant increased sensitivity to low dose angiotensin II (3 and 10 μg/kg) compared with wild-type littermates (Fig. 4*A*, *captopril*). In making another attempt to clarify a role of APJ in blood pressure regulations, we generated double knock-out mice for *APJ* and *AT1a* by crossing *APJ*-deficient and AT1a-deficient mice. As shown in Fig. 4*B*, AT1a-deficient mice displayed marked hypotension compared with that of wild-type mice as described previously (11). Under the attenuated conditions to the vasopressor actions on the AT1a-deficient background, the base-line blood pressure of double mutant mice homozygous for both *APJ* and *AT1a* was elevated significantly compared with that of AT1a-deficient mice (81.6 ±

4.0 and 75.8 ± 2.3 mm Hg, respectively; $p < 0.05$). These data indicated that APJ has a potential ability to lower the blood pressure. Previously, it was demonstrated that AT2-deficient mice exhibited the increase in sensitivity to low dose angiotensin II-induced vasopressor action (26, 27). Likewise, APJ may function as a member of the vasorelaxation system in blood pressure regulation against the vasoconstriction system including angiotensin II-induced AT1 signaling.

In conclusion, the inactivation of the *APJ* gene in mice by gene targeting indicated that this receptor is responsible for the hypotensive effect of apelin in adult mice *in vivo* and plays a counterregulatory role against vasopressor stimulation. In addition, by using primary endothelial cells derived from mice, it is suggested that the hypotensive effect induced by apelin-APJ signaling is mediated through the NO/L-arginine system activated by eNOS phosphorylation. In the future, beside the systemic effects of apelin-APJ signaling, the selective functions of APJ in the local tissues including the central nervous and cardiovascular systems should be elucidated. This animal model may be useful for investigating the *in vivo* role of apelin-APJ signaling in normal and pathophysiological conditions and for testing pharmacotherapeutic implications for the cardiovascular diseases.

Acknowledgments—We thank Dr. Shin-ichiro Nishimatsu and the Fukamizu laboratory members for helpful discussion and encouragement.

REFERENCES

1. O'Dowd, B. F., Heiber, M., Chan, A., Heng, H. H., Tsui, L. C., Kennedy, J. L., Shi, X., Petronis, A., George, S. R., and Nguyen, T. (1993) *Gene (Amst.)* **136**, 355–360
2. Tatemoto, K., Hosoya, M., Habata, Y., Fujii, R., Kakegawa, T., Zou, M. X., Kawamata, Y., Fukusumi, S., Hinuma, S., Kitada, C., Kurokawa, T., Onda, H., and Fujino, M. (1998) *Biochem. Biophys. Res. Commun.* **251**, 471–476
3. Hosoya, M., Kawamata, Y., Fukusumi, S., Fujii, R., Habata, Y., Hinuma, S., Kitada, C., Honda, S., Kurokawa, T., Onda, H., Nishimura, O., and Fujino, M. (2000) *J. Biol. Chem.* **275**, 21061–21067
4. Kawamata, Y., Habata, Y., Fukusumi, S., Hosoya, M., Fujii, R., Hinuma, S., Nishizawa, N., Kitada, C., Onda, H., Nishimura, O., and Fujino, M. (2001) *Biochim. Biophys. Acta* **1538**, 162–171
5. Reaux, A., De Mota, N., Skultetyova, I., Lenkei, Z., El Messari, S., Gallatz, K., Corvol, P., Palkovits, M., and Llorens-Cortes, C. (2001) *J. Neurochem.* **77**, 1085–1096
6. Medhurst, A. D., Jennings, C. A., Robbins, M. J., Davis, R. P., Ellis, C., Winborn, K. Y., Lawrie, K. W., Hervieu, G., Riley, G., Bolaky, J. E., Herrity, N. C., Murdock, P., and Darker, J. G. (2003) *J. Neurochem.* **84**, 1162–1172
7. Lee, D. K., Cheng, R., Nguyen, T., Fan, T., Kariyawasam, A. P., Liu, Y., Osmond, D. H., George, S. R., and O'Dowd, B. F. (2000) *J. Neurochem.* **74**, 34–41
8. Tatemoto, K., Takayama, K., Zou, M. X., Kumaki, I., Zhang, W., Kumano, K., and Fujimiya, M. (2001) *Regul. Pept.* **99**, 87–92
9. Cheng, X., Cheng, X. S., and Pang, C. C. (2003) *Eur. J. Pharmacol.* **470**, 171–175
10. Katugampola, S. D., Maguire, J. J., Matthewson, S. R., and Davenport, A. P. (2001) *Br. J. Pharmacol.* **132**, 1255–1260
11. Sugaya, T., Nishimatsu, S., Tanimoto, K., Takimoto, E., Yamagishi, T., Imamura, K., Goto, S., Imaizumi, K., Hisada, Y., Otsuka, A., Uchida, H., Sugiura, M., Fukuta, K., Fukamizu, A., and Murakami, K. (1995) *J. Biol. Chem.* **270**, 18719–18722
12. Yagi, T., Nada, S., Watanabe, N., Tamemoto, H., Kohmura, N., Ikawa, Y., and Aizawa, S. (1993) *Anal. Biochem.* **214**, 77–86
13. Yagi, T., Tokunaga, T., Furuta, Y., Nada, S., Yoshida, M., Tsukada, T., Saga, Y., Takeda, N., Ikawa, Y., and Aizawa, S. (1993) *Anal. Biochem.* **214**, 70–76
14. Goto, Y., Sugiyama, F., Tanimoto, K., Ishida, J., Syoji, M., Takahashi, A., Sugiyama, Y., Murakami, K., Fukamizu, A., and Yagami, K. (1995) *Lab. Anim. Sci.* **45**, 601–603
15. Chomczynski, P., and Sacchi, N. (1987) *Anal. Biochem.* **162**, 156–159
16. Miyagishi, M., Nakajima, T., and Fukamizu, A. (2000) *Int. J. Mol. Med.* **5**, 27–31
17. Fukamizu, A., Sugimura, K., Takimoto, E., Sugiyama, F., Seo, M. S., Takahashi, S., Hatae, T., Kajiwara, N., Yagami, K., and Murakami, K. (1993) *J. Biol. Chem.* **268**, 11617–11621
18. Taheri, S., Murphy, K., Cohen, M., Sujkovic, E., Kennedy, A., Dhillo, W., Dakin, C., Sajedi, A., Ghatei, M., and Bloom, S. (2002) *Biochem. Biophys. Res. Commun.* **291**, 1208–1212
19. Szokodi, I., Tavi, P., Foldes, G., Voutilainen-Myllyla, S., Ilves, M., Tokola, H., Pikkarainen, S., Piuhola, J., Rysa, J., Toth, M., and Ruskoaho, H. (2002) *Circ. Res.* **91**, 434–440
20. Foldes, G., Horkay, F., Szokodi, I., Vuolteenaho, O., Ilves, M., Lindstedt, K. A., Mayranpaa, M., Sarman, B., Seres, L., Skoumal, R., Lako-Futo, Z., deChatel, R., Ruskoaho, H., and Toth, M. (2003) *Biochem. Biophys. Res. Commun.* **308**, 480–485
21. Chen, M. M., Ashley, E. A., Deng, D. X., Tsalenko, A., Deng, A., Tabibiazar, R., Ben-Dor, A., Fenster, B., Yang, E., King, J. Y., Fowler, M., Robbins, R., Johnson, F. L., Bruhn, L., McDonagh, T., Dargie, H., Yakhini, Z., Tsao, P. S., and Quertermous, T. (2003) *Circulation* **108**, 1432–1439
22. Vickers, C., Hales, P., Kaushik, V., Dick, L., Gavin, J., Tang, J., Godbout, K., Parsons, T., Baronas, E., Hsieh, F., Acton, S., Patane, M., Nichols, A., and Tummino, P. (2002) *J. Biol. Chem.* **277**, 14838–14843
23. Michell, B. J., Griffiths, J. E., Mitchelhill, K. I., Rodriguez-Crespo, I., Tiganis, T., Bozinovski, S., de Montellano, P. R., Kemp, B. E., and Pearson, R. B. (1999) *Curr. Biol.* **9**, 845–848
24. Fulton, D., Gratton, J. P., McCabe, T. J., Fontana, J., Fujio, Y., Walsh, K., Franke, T. F., Papapetropoulos, A., and Sessa, W. C. (1999) *Nature* **399**, 597–601
25. Dimmeler, S., Fleming, I., Fisslthaler, B., Hermann, C., Busse, R., and Zeiher, A. M. (1999) *Nature* **399**, 601–605
26. Hein, L., Barsh, G. S., Pratt, R. E., Dzau, V. J., and Kobilka, B. K. (1995) *Nature* **377**, 744–747
27. Ichiki, T., Labosky, P. A., Shiota, C., Okuyama, S., Imagawa, Y., Fogo, A., Niimura, F., Ichikawa, I., Hogan, B. L., and Inagami, T. (1995) *Nature* **377**, 748–750

ELSEVIER

Eur. J. Cell Biol. 83 (2004); 555–565
http://www.elsevier.de/ejcb

EJCB

Syntrophin is an actin-binding protein the cellular localization of which is regulated through cytoskeletal reorganization in skeletal muscle cells

Yuko Iwata[1)a], Maurilio Sampaolesi[a], Munekazu Shigekawa[b], Shigeo Wakabayashi[a]

[a] Department of Molecular Physiology, National Cardiovascular Center Research Institute, Suita, Osaka, Japan
[b] Department of Human Life Sciences, Senri Kinran University, Suita, Osaka, Japan

Received May 5, 2004
Received in revised version August 5, 2004
Accepted August 6, 2004

Syntrophin; Actin binding; F-actin; Translocation; Skeletal muscle; Myotube

We have characterized the interaction of syntrophin with F-actin. Subcellular fractionation of cardiac and skeletal muscle tissues showed that α-, β_1- and β_2-syntrophins were present in the soluble and the membrane fraction. Syntrophins are known to bind to the dystrophin-glycoprotein complex (DGC), but since the DGC is not present in the soluble fraction, it was concluded that some syntrophin did not associate with the DGC. Native syntrophins purified from the soluble fraction and recombinant syntrophins were both able to bind to F-actin, and binding occurred through several sites on syntrophin, including the second pleckstrin homology domain and the unique carboxyl-terminal domain. Syntrophin was also able to inhibit actin-activated myosin ATPase activity and actomyosin super-precipitation. α-Syntrophin co-localized with cortical F-actin fibers when expressed in Chinese hamster ovary cells, and deletion of the actin-binding region abolished co-localization. Most of exogenous or endogenous syntrophin also co-localized with stress fibers in endothelial and smooth muscle (A7r5) cells. However, syntrophins were mostly localized in the cytosol of serum-starved C2C12 or primary cultured skeletal muscle myotubes, and translocated to the membrane upon treatment with lysophosphatidic acid or the actin-stabilizing agent jasplakinolide. The actin-depolymerizing agent latrunculin-B abolished this syntrophin translocation. These findings suggest that syntrophin is an actin-binding protein the subcellular localization of which is regulated through cytoskeletal reorganization.

[1)] **Corresponding author:** Dr. Yuko Iwata, Department of Molecular Physiology, National Cardiovascular Center Research Institute, Fujishiro-dai 5–7, Suita, Osaka 5658565, Japan, e-mail: yukoiwat@ri.ncvc.go.jp, Fax: +81668355314.

Abbreviations. CHO Chinese hamster ovary. – DAP Dystrophin-associated protein. – DG Dystroglycan. – DGC Dystrophin-glycoprotein complex. – GFP Green fluorescent protein. – JAS Jasplakinolide. – Lat B Latrunculin B. – LPA Lysophosphatidic acid. – MBP Maltose-binding protein. – PCR Polymerase chain reaction. – SG Sarcoglycan.

Introduction

Mutations in several components of the dystrophin-glycoprotein complex (DGC) are known to be involved in the pathogenesis of muscular dystrophies, including cardiomyopathy (Straub and Campbell, 1997; Ozawa et al., 1998; Towbin and Bawles, 2002). The intracellular part of the DGC is formed by the membrane-associated cytoskeletal protein dystrophin, the protein product of the Duchenne muscular dystrophy (DMD) gene. Dystrophin is localized at the inner surface of the peripheral sarcolemma of skeletal muscle cells, forming a submembrane cytoskeletal network. The C-terminal domains of multiple dystrophins in this network form tight complexes with several dystrophin-associated proteins (DAPs), including peripheral membrane syntrophins and intrinsic membrane glycoproteins (including α-, β-, γ-, and δ-sarcoglycans (SG), β-dystroglycan (DG) and the non-glycosylated intrinsic membrane protein sarcospan), and the extracellular laminin-binding glycoprotein α-DG (Tinsley et al., 1994; Campbell, 1995). These DAPs link dystrophin to the sarcolemma and to the extracellular matrix, and because the N-terminal domain of dystrophin binds to actin (Rybakova et al., 1996), dystrophin also serves to connect the actin cytoskeleton with the extracellular matrix.

Syntrophin is an important component of the DGC that is essential for the maintenance of integrity of the sarcolemma. To date, five syntrophin isoforms α, β1, β2, γ1, and γ2 have been

0171-9335/04/083/10-555 $30.00/0

identified (Ahn et al., 1996; Piluso et al., 2000). It has been shown that α-, β1- and β2-syntrophin are expressed in striated muscles (Ahn et al., 1996), while γ1-syntrophin is expressed uniquely in the brain and γ2-syntrophin is somewhat broadly expressed (Piluso et al., 2000). Each syntrophin is encoded by a separate gene, but the proteins share a common domain organization. Each contains two tandem pleckstrin homology (PH) domains at the amino-terminus, a single PDZ domain, and a highly conserved carboxyl-terminal syntrophin-unique (SU) region (Ahn et al., 1996; Piluso et al., 2000), suggesting multiple roles in anchoring proteins at the membrane through the PDZ domain and in signal transduction. Syntrophins bind directly to dystrophin, utrophin and dystrobrevin, through an interaction mediated by the second PH domain and the SU domain (Kachinsky et al. 1999). The first PH domain of α-syntrophin can bind phosphatidylinositol lipids (Chockalingam et al., 1999), thus providing an additional mode of membrane interaction. The PDZ domain of syntrophin binds to a variety of molecules, including sodium channels (Gee et al., 1998), neuronal nitric oxide synthase (nNOS) (Brenman et al., 1996), serine/threonine kinases (Lumeng et al., 1999) and stress-activated protein kinase-3 (Hasegawa et al., 1999). Thus, syntrophin is thought to link several signaling proteins to the actin cytoskeleton and to the extracellular matrix via dystrophin. However, the precise function of syntrophins is currently unknown. Recent α-syntrophin-knockout studies show that α-syntrophin plays important roles in muscle regeneration (Hosaka et al., 2002), in neuromuscular maturation (Adams et al., 2000, Kameya et al., 1999) and in water transport (Amiry-Moghaddam et al., 2003).

We have previously shown that syntrophin binds to actin and calmodulin, and we roughly identified the binding regions for these accessory proteins using recombinant α-syntrophin (Iwata et al., 1998). In the present study we have further characterized the interaction of syntrophin with F-actin. Unexpectedly, we found that some syntrophin molecules do not form a complex with the DGC and are recovered in the soluble fraction of cardiac and skeletal muscle proteins. Furthermore, while exogenously expressed α-syntrophin co-localized with cortical F-actin fibers in non-muscle cells, endogenous syntrophin was partly localized in the cytosol in cultured skeletal muscle cells. Interestingly, syntrophin is translocated to the peripheral region of skeletal muscle cells upon stimulation of cells with lysophosphatidic acid (LPA), or upon treatment with actin-stabilizing agents. These findings provide new insights into the function of syntrophin as an actin-binding protein.

Materials and methods

Plasmid construction and purification of proteins from *Escherichia coli*

The cDNA coding for rabbit α-syntrophin was isolated by reverse transcriptase-polymerase chain reaction (RT-PCR) using total RNA prepared from rabbit skeletal muscle. All constructs were produced by means of a PCR-based strategy. The PCR products containing various regions of α-syntrophin were inserted into appropriate restriction sites of the pCDNA3.1 (+) vector (Invitrogen, Carlsbad, CA, USA) or pGFP-C1 expression vectors (Clontech, Palo Alto, CA, USA). Various fusion proteins of α-syntrophin with maltose-binding protein were purified from transformed *E. coli*, according to the manufacturer's protocol, after construction in the pMAL-c vector (New England Biolabs, Hitchi, UK).

Preparation of actin and myosin, and measurement of actin-activated myosin ATPase

Actin was purified from rabbit skeletal muscle acetone powder, as described by Spudich and Watt (1974). Rabbit skeletal muscle myosin was prepared according to the method of Perry (1955). For measurement of actin-activated myosin ATPase, various amounts of recombinant syntrophin were added to a solution containing 1 mM ATP, 2.4 mM $MgCl_2$, 40 mM KCl, 7 mM PIPES (pH 6.9) and F-actin (final concentration 150 μg/ml), and incubated for 5 min at 25°C. The ATPase reaction was started by adding myosin (final concentration 60 μg/ml), and stopped 10 min later by adding 5% trichloroacetic acid. The amount of inorganic phosphate liberated was determined by the malachite green method (van Veldhoven and Mannaerts, 1987).

F-actin co-sedimentation and superprecipitation assays

F-actin (2.5 μM) was incubated for 30 min at room temperature with various concentrations of recombinant syntrophin/MBP fusion proteins in 60 μl of actin-binding buffer (1 mM ATP, 0.2 mM $CaCl_2$, 2 mM $MgCl_2$, 100 mM NaCl, 0.5 mM β-mercaptoethanol and 2 mM Tris/HCl, pH 8.0), and then subjected to centrifugation at 100,000g for 40 min. Pellets were redissolved in an equivalent volume of actin-binding buffer and co-sedimentation of syntrophin was detected by Coomassie Brilliant Blue (CBB) staining after sodium dodecyl sulfate-polyacrylamide gel electrophoresis (SDS-PAGE). Superprecipitation of actomyosin was followed by measuring the increase in turbidity. Various concentrations of syntrophin were incubated for 5 min in 1.7 mM ATP, 5 mM $MgCl_2$, 40 mM KCl, 1 mM EDTA, 7 mM PIPES (pH 6.9) containing 160 μg/ml muscle F-actin at 25°C, and absorbance at 660 nm was monitored after the addition of 240 μg/ml myosin.

Cell culture and plasmid transfection

C2C12 cells were grown on 100-mm tissue culture dishes in DMEM supplemented with 10% heat-inactivated fetal calf serum (FCS) at 37°C in the presence of 5% CO_2. When the cells reached confluence, the growth medium was replaced with DMEM containing 5% horse serum to induce myotube differentiation. Seven to ten days after medium replacement, 90% of the cells had fused to form myotubes. CHO, bovine endothelial and A7r5 cells were cultured similarly in DMEM containing 10% fetal calf serum. The primary culture of myoblasts from skeletal muscles and myotube differentiation were done as described before (Sampaolesi et al., 2001). Briefly, satellite cells were isolated from gastrocnemius muscles of hamster by enzymatic dissociation and cultured in Ham's F12 medium supplemented with 20% FCS and 2.5 ng/ml bFGF (Promega BRL, Madison, Wisconsin) and 1% chick embryo extract (GIBCO BRL). After passage with trypsinization followed by culture during 1–2 days, medium was changed to DMEM (GIBCO BRL) containing 2% horse serum (Hyclone Laboratories, Logan, UT) to initiate differentiation. Myoblasts started to fuse and form myotubes in culture within 24 h. Three to five days after medium replacement, myotubes were subjected to immunohistochemical analysis. For some experiments (see Fig. 5), horse serum was removed overnight after myotube formation. Various syntrophin constructs were transfected into CHO or bovine endothelial cells using lipofectin (Invitrogen). After selection with G418 (Sigma Chemicals Co., St. Louis, MO, USA), individual colonies expressing exogenous syntrophins were isolated.

Immunohistochemistry

Adherent cells were fixed in 2% paraformaldehyde for 15 min, and either analyzed for GFP expression immediately on confocal fluorescence microscope as described previously (Yoshida et al., 1998).

Antibody production

A monoclonal antibody (anti-pan-syn) against syntrophin was produced by immunizing mice with a fraction eluted with N-acetyl glucosamine (NAG) from succinylated wheat germ agglutinin (WGA), as described previously (Iwata et al., 1996). This antibody recognizes all three isoforms of syntrophin (α, β1 and β2) because it reacts with the PDZ domain of syntrophin, which is common to these isoforms. The other monoclonal anti-syntrophin antibody SYN1351, which recognizes all three isoforms of syntrophin, was a gift from Dr. Stanley C. Froehner. A polyclonal antibody against α-syntrophin was produced by immunizing rabbits with the peptide RQPSSPGPQPRNLSEA as described previously (Ahn et al., 1996). This antibody specifically recognizes α-syntrophin. Purified antibodies (anti-pan-syn and anti-α-syn) were coupled to activated aldehyde on agarose (Actigel, Sterogene, CA, USA) to prepare immunoaffinity adsorbents. Rabbit polyclonal antibodies p50 and p43 against rabbit α-SG and β-DG, respectively, have been described previously (Iwata et al., 1996). A mouse monoclonal antibody against α-actin was purchased from BioMaker (Rehovot, Israel). Mouse monoclonal antibodies against dystrophin (NCL-Dys1 and NCL-Dys2) were purchased from Novocastra Laboratories (Newcastle, UK).

Subcellular fractionation and purification of native syntrophin from muscles

Cardiac and skeletal muscles (1 g) from normal hamsters were homogenized with a Physcotron three times for 30 s in 1 ml of 10 mM $NaHCO_3$ and centrifuged at 5500g (max) for 10 min. After centrifugation of the supernatant at 480,000g (max) for 40 min, the high-speed supernatant (soluble fraction) and the precipitate (membrane fraction) were subjected to SDS-PAGE. For subcellular fractionation from cultured myotubes (see Fig. 6B), homogenates were directly applied to high-speed centrifugation. Proteins were blotted onto Immobilon membranes and then immunostained with anti-dystrophin, anti-pan-syntrophin and anti-β-DG antibodies, respectively. For purification of native syntrophin, proteins extracted from rabbit ventricles using low-ionic-strength solutions were applied to a DEAE-cellulose column, and the flow-through fraction was subjected to heparin-Sepharose chromatography. The bound proteins were eluted with a linear gradient of NaCl, and the fractions containing 59-kDa proteins were pooled.

Other procedures

Quantitative immunoblot analysis and immunocytochemistry were performed as described previously (Tawada-Iwata et al., 1993). Muscle homogenate preparation (Tawada-Iwata et al., 1993), purification of the dystrophin complex (Tawada-Iwata et al., 1993), and the calmodulin-Sepharose binding experiment (Iwata et al., 1998) were performed as described in detail previously. Protein concentrations were measured using a bicinchoninic acid assay system (Pierce Chemical Co., Rockford, USA) with bovine serum albumin as a standard.

Results

Syntrophin exists in both soluble and membrane fractions from cardiac and skeletal muscles

We have previously reported that the actomyosin fraction prepared from cardiac or skeletal muscles contain proteins recognized by an anti-syntrophin antibody (Iwata et al., 1998). In this study, in order to avoid contamination with contractile proteins, we homogenized the tissues in a low-salt buffer and separated the soluble and membrane fractions after high-speed centrifugation. Immunoblot analysis showed that both the membrane and soluble fractions from cardiac or skeletal muscles contained 59- and 60–62-kDa proteins recognized by the anti-syntrophin antibody (Fig. 1A, IB: syn). In contrast, β-DG was present exclusively in the membrane fraction. We determined that the 59- and 60–62-kDa proteins were α- and β1/β2-syntrophin, respectively, by immunoblotting with isoform-specific antibodies (data not shown). As syntrophins are

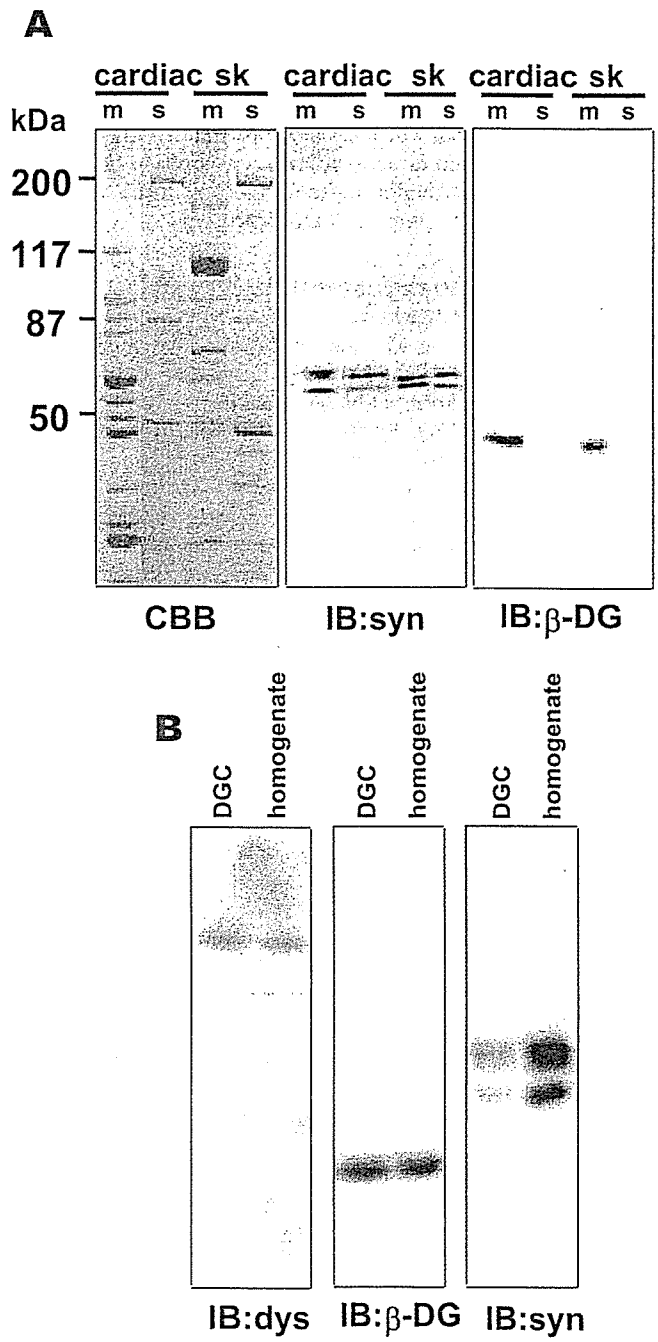

Fig. 1. Subcellular fractionation of cardiac and skeletal muscles. (A) Cardiac and skeletal muscles from hamsters were homogenized and fractionated as described in Materials and methods. The membrane (m) and soluble (s) fractions were subjected to SDS-PAGE on a 7.5% gel. Proteins were stained with CBB or immunostained with anti-pan-syntrophin (syn) and anti-β-DG antibodies. (B) Purified DGC and initial homogenate were subjected to SDS-PAGE. Proteins were immunostained with anti-dystrophin (dys), anti-β-DG and anti-pan-syntrophin antibodies (syn), respectively. In the second and third panels, proteins from the DGC fraction and the homogenate were applied to the gel so that amounts of dystrophin were the same on the immunoblot.